

Review

Corrosion-Resistant Coating Based on High-Entropy Alloys

Cheng Lin ^{1,2}  and Yonggang Yao ^{1,*} 

¹ State Key Laboratory of Materials Processing and Die and Mould Technology, School of Materials Science and Engineering, Huazhong University of Science and Technology, Wuhan 430074, China

² School of Materials Science and Engineering, Northeastern University, Shenyang 110819, China

* Correspondence: yaoyg@hust.edu.cn

Abstract: Metal corrosion leads to serious resource waste and economic losses, and in severe cases, it can result in catastrophic safety incidents. As a result, proper coatings are often employed to separate metal alloys from the ambient environment and thus prevent or at least slow down corrosion. Among various materials, high-entropy alloy coatings (HEA coating) have recently received a lot of attention due to their unique entropy-stabilized structure, superior physical and chemical properties, and often excellent corrosion resistance. To address the recent developments and remaining issues in HEA coatings, this paper reviews the primary fabrication methods and various elemental compositions in HEA coatings and highlights their effects on corrosion resistance properties. It is found that FeCoCrNi-based and refractory high-entropy alloy coatings prepared by the laser/plasma cladding method typically show better corrosion resistance. It also briefly discusses the future directions toward high-performing corrosion-resistant coatings based on HEA design.

Keywords: high-entropy alloy; coating; corrosion resistance; coating fabrication



Citation: Lin, C.; Yao, Y.

Corrosion-Resistant Coating Based on High-Entropy Alloys. *Metals* **2023**, *13*, 205. <https://doi.org/10.3390/met13020205>

Academic Editor: Sundeep Mukherjee

Received: 28 December 2022

Revised: 16 January 2023

Accepted: 18 January 2023

Published: 20 January 2023



Copyright: © 2023 by the authors. Licensee MDPI, Basel, Switzerland. This article is an open access article distributed under the terms and conditions of the Creative Commons Attribution (CC BY) license (<https://creativecommons.org/licenses/by/4.0/>).

1. Introduction

High-entropy alloys (HEAs) [1–3], originally proposed in 2004, have received a great deal of attention from scholars around the world. The traditional one-dominant component alloy design concept is subverted by this nearly iso-molar ratio multi-principal HEA design, which brings alloys into the gigantic multidimensional composition space. HEAs have been loosely defined as alloys containing at least five major elements with an average atomic percentage (at.%) between 5% and 35% for each element. Since then, this new alloy design strategy has created a field with enormous potential for multicomponent alloys [4,5]. For instance, the design of five- to thirteen-member alloys using 13 commonly used metallic elements in the periodic table would create more than 7000 alloys. Additionally, the HEAs demonstrated some unprecedented success owing to the entropy-stabilized structure, severe lattice distortion, kinetic hysteresis diffusion, and high-entropy mixing-induced cocktail effect [6,7]. As a result, HEAs have not only excellent mechanical properties, such as high strength, hardness, wear resistance, and superior compression [8–11], but also good physical and chemical properties, such as corrosion resistance, catalytic properties, thermoelectric properties, etc. [12–17].

In addition to bulk HEAs, many people are now studying coating because the special and excellent structure of HEAs can significantly improve the anti-corrosion performance of various metals and their service performance in various extreme conditions. HEA coatings have a similar composition design concept as HEAs but very different fabrication processes due to the 2D thin film geometry. In addition, due to the unique structure, the resultant mechanical properties and failure mechanism of HEA coatings are also largely different from bulk HEAs [18,19]. Particularly, HEA coating can resolve some structural and performance disadvantages in bulk HEAs. Some advantages of HEA coating are listed below.

- Lower cost. Due to the complexity of the alloy composition and the large differences between the melting points of the elements in HEAs, significant elemental segregation occurs during melt solidification and cooling [20], and post-treatment is required to obtain well-organized HEAs [21–23], leading to complicated preparation and high cost. In addition, adding expensive elements such as Nb, Cr, V, Ni, Ti, and Co to the HEAs [24–26] means that the material cost of bulk HEAs is very high, and it is difficult to achieve industrial-wide application. In contrast, HEA coating requires significantly fewer materials (thin films) and has many energy-efficient fabrication methods to ensure HEA formation, thus saving both material and fabrication costs to enable industrial adoption;
- Flexible preparation. In recent years, various processes have successfully fabricated HEA coatings with excellent properties, including laser cladding, magnetron sputtering, and thermal spray. The micro properties (such as microstructure and phase composition) and the macro properties of the coating (such as thickness, density, flatness, surface quality, etc.) can be flexibly controlled by adjusting the process parameters during coating preparation (such as scanning speed, laser power, deposition temperature, sputtering power, etc.);
- Wide applicability. Several common elements employed in HEA coatings (such as Al, Fe, Ti, Cr, Ni, etc.) can significantly improve the service life of the substrate and the performance of the product, particularly for common steel, Al alloy, Mg alloy, Ti alloy, and other substrates. Additionally, because of the characteristics of the coating that has been prepared on the substrate surface, it can be applied to substrate materials with a variety of shapes to ensure that each part's thickness is approximately uniform and that the overall performance is relatively steady;
- Excellent properties. The corrosion resistance, erosion resistance, friction, and wear properties of the coating have received increasing focus since the corrosion process is characterized by its surface reaction. HEA coatings have been regarded as a solution to satisfy a range of serious service conditions, such as marine corrosion, extreme cold corrosion, plateau corrosion, nuclear radiation corrosion, and other corrosive environments.

Figure 1 shows the preparation process, typical microstructure, and respective advantages and disadvantages of bulk HEA and HEA coatings.

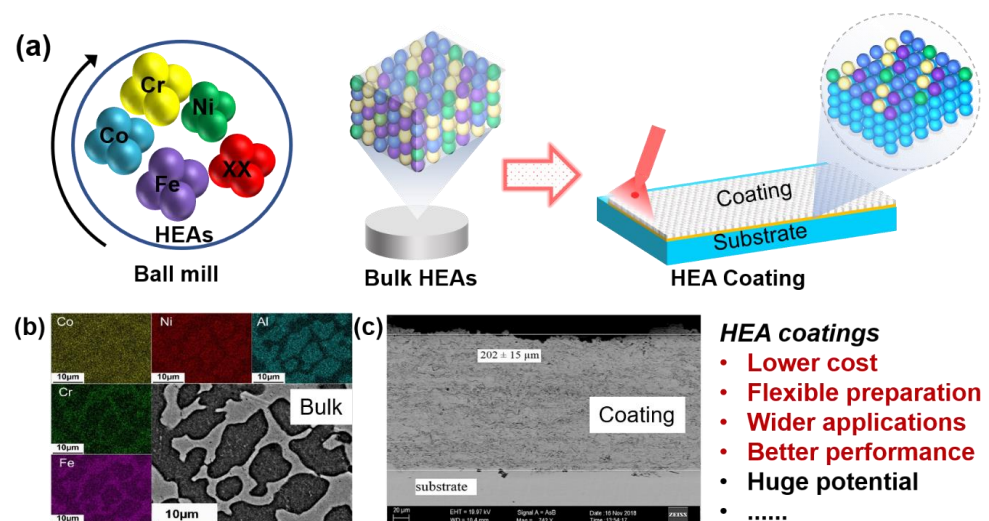


Figure 1. Bulk HEAs and HEA coating. (a) Schematic of bulk HEAs and HEA coatings. (b) EDS map of Al-Co-Cr-Fe-Ni bulk HEA [27]. Copyright 2021 Elsevier. (c) Cross-sectional back scattered micrograph of the FeCoCrNi₂Al HEA-coated steel [28]. Copyright 2019 Elsevier.

This article will review the preparation processes, excellent properties, and failure mechanism of HEA coatings in the corrosion process, and look forward to new strategies to prepare HEA coatings with further improved properties, aiming to provide methodological ideas to understand HEA coatings in terms of preparation, composition, structure, and properties.

2. Review

2.1. Current Situation of HEA Coating

More stringent performance standards for the materials used, including corrosion resistance [29], friction and wear resistance [30], high-temperature oxidation resistance [31], high strength [32], etc., have been proposed as a result of mankind's ongoing exploration in the fields of aerospace, shipping and maritime, rail transportation, pipeline engineering, and new energy. The surface of the materials used must have excellent corrosion resistance, scouring resistance, and other features, especially in the fields of deep-sea corrosion and high-temperature erosion.

Anti-corrosion coatings for metal-based materials can be simply classified into the following four categories: metallic coatings, diffusion coatings, organic coatings, and ceramic coatings. In addition to HEA coating, common metallic coatings can be simply divided into Ni-Co-based coatings, amorphous coatings, metal-based composite coatings, etc. Diffusion coating refers to the diffusion of certain elements into the substrate, and there is a strong metallurgical bond with the substrate, with high adhesion strength [33]. Organic coating is a kind of environmental protection and an excellent corrosion resistance coating, which is widely used in industrialization [34]. Organic coatings are currently classified as conductive polymer coatings, shielding polymer coatings, and smart coatings. Ceramic coatings are inorganic non-metallic materials synthesized by high-temperature processing, which combine the toughness and bending resistance of metals with the high-temperature resistance, high strength, and oxidation resistance of ceramics to improve the performance of coatings [35]. Table 1 summarizes the advantages and disadvantages of different types of coatings for a simple comparison.

Table 1. Comparison of different types of coatings.

Type	Advantages	Disadvantages
Common metallic coatings	Proven and simple process Excellent corrosion and friction resistance Excellent electrochemical properties	Not environmentally friendly Expensive alloying elements Co/Ni
Diffusion coatings	High-temperature resistant Fast preparation speed Uniform coating thickness	Processes are difficult to be controlled High preparation cost Limitations in the coating composition
Organic coatings	Protecting the environment Excellent physical and chemical properties Excellent physical barrier function	Difficult to achieve large-scale production Not resistant to high temperatures
Ceramic coatings	Excellent mechanical and tribological properties Can be compounded with other coatings	Prone to defects such as porosity and cracks Poor toughness
HEA coatings	Multi-performance Suitable for a wide range of service conditions	Difficult to design components Process limitations Theoretical research needs to be improved

The service performance and life of materials with a variety of applications may now be greatly increased with the use of coating technology, which is now widely acknowledged as an efficient method. Laser melting, magnetron sputtering, and thermal spray are the principal methods used to produce coatings [36–38]. The performance of the material surface is enhanced by the preparation of the coating materials, which mostly involve laser melting, magnetron sputtering, and thermal spray. The preparation of high-performance coating materials is usually achieved based on the study of the properties of the bulk system and the advanced methods of surface technology [39]. Due to the thinness of HEA

coatings, different techniques are often used based on the prepared layer thickness. For instance, physical vapor deposition techniques (such as magnetron sputtering) can be used to create coatings from submicron to micron thickness, whereas laser cladding or thermal spray techniques can be used to create coatings thicker than micron thickness. They will cool quickly during this time, increasing the nucleation rate and causing the formation of fine grains while tending to suppress phase separation, resulting in a supersaturated state and the strengthening mechanisms of conventional alloys such as solid solution strengthening and fine-grain strengthening. The deposition process of HEA coatings, in contrast to conventional alloys, includes several elements that have hysteresis diffusion effects that may enhance the effects of rapid cooling. Typically, these effects provide a reduction in the rate of grain and phase coarsening and a delay in the crystallization of amorphous structures at high temperatures. Therefore, compared to traditional alloy coatings, fine-grain strengthening and second-phase strengthening are significantly more effective at the same cooling rate. Additionally, the microstructure and properties of HEA coatings are influenced in distinct ways by high-entropy effects and severe lattice distortion effects, which may be advantageous for particular applications [40,41]. It is worth noting that the production mechanism of HEAs is still unclear; hence, it is debatable and subject to additional study whether the past studies on high-entropy bulk alloys are fully applicable to high-entropy coatings or thin films.

As shown in Figure 2, based on a variety of coatings being researched for application in multiple service contexts currently, high-entropy coatings can be broadly divided into three categories [42].

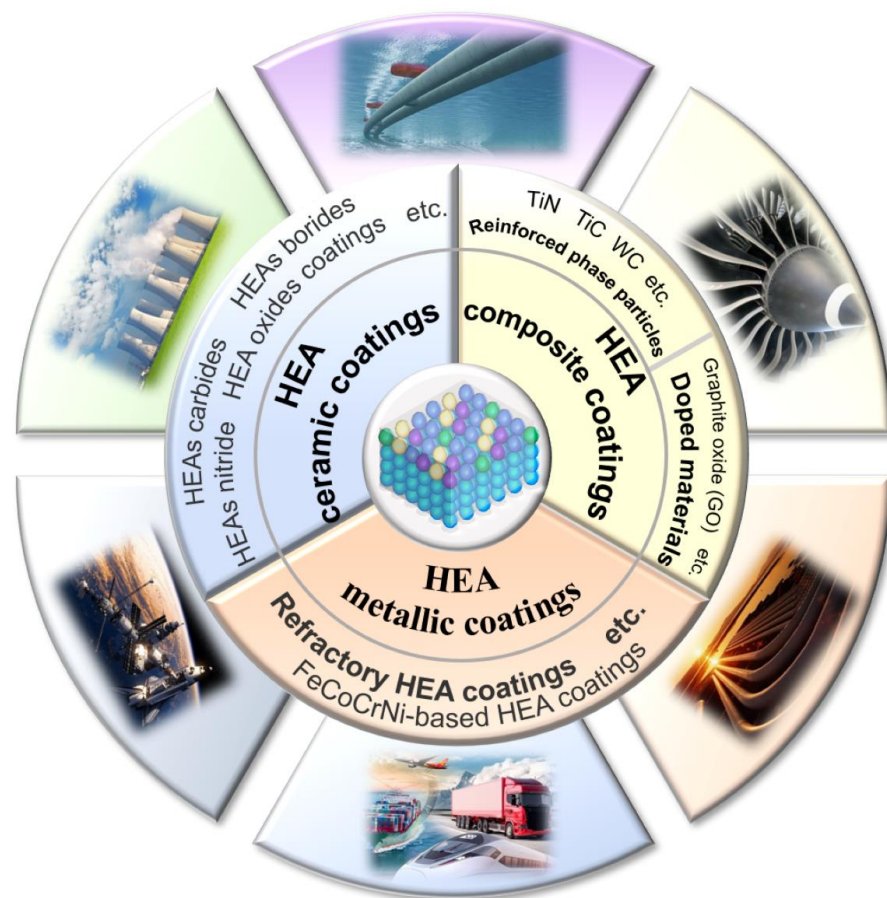


Figure 2. Classification of HEA coating. Based on the compositions and applications of HEA coatings, it is divided into metallic coatings, composite coatings, and ceramic coatings.

1. HEA metallic coatings, such as refractory high-entropy coatings and coatings based on transition metals; the FeCoCrNi-based HEA coating is a typical HEA metal coating with excellent corrosion resistance due to the Cr and Ni elements, which are the main elements that improve the corrosion resistance in the alloys by encouraging the forming of a passive film.
2. High-entropy ceramic coatings, such as covalent and ion-bonded high-entropy ceramic coatings, are made by combining HEAs with N [2], B [43], C [44], O [45], and other anions. The typical corrosion-resistant high-entropy ceramic coating is nitride coating because chemically inert transition metal nitrides (such as CrN or TiN) are beneficial to improving coatings' corrosion resistance.
3. HEA composite coatings. A HEA can be used as a matrix or binder for ceramics or as a reinforcing material for light alloys such as aluminum and magnesium alloys. The reinforced phase particles (TiN [46], TiC [47], etc.) and doped materials (graphite oxide (GO) [48], etc.) are often compounded.

Typical wear-resistant coatings include iron-based coatings, nickel-based coatings, metal–ceramic composite coatings, HEA coatings, and amorphous alloy coatings, etc.; common corrosion-resistant coatings include various amorphous alloy coatings and HEA coatings. Due to their notable benefits in wear resistance and corrosion resistance, HEA coatings are one of those that have recently caught the attention of scholars.

2.2. Fabrication Methods of HEA Coatings

In recent years, a variety of HEA coatings have been successfully prepared by magnetron sputtering, laser cladding, thermal spray, electrochemical deposition, etc. Most of the high-entropy coatings have a relatively uniform and dense microstructure, good thermal stability, and wear resistance. Porosity is a key factor in determining the corrosion resistance and wear resistance of coatings, and a suitable preparation method can determine the size of porosity. The two most popular preparation techniques for enhancing the corrosion resistance of HEA coatings are laser cladding and magnetron sputtering. In light of the issues with the currently available technologies, this paper will concentrate on these two fabrication methods, provide a brief overview and summary of other fabrication methods, and consider potential future new research directions and ideas for the fabrication of high-entropy coatings.

2.2.1. Laser Cladding

With laser cladding, the powder is synchronously fed to the cladding zone or pre-set on the substrate while being protected by an atmosphere. The coating is then formed by sweeping a high-energy beam across the surface being highly supercooled, and the coating thickness can be adjusted between microns and millimeters. Its advantages mainly include high energy density, minimal thermal impact on the substrate, low dilution of the substrate, and quick heating and cooling. The created high-entropy layer establishes a solid metallurgical link with the substrate and has a more uniform, dense microstructure with fewer macroscopic and microscopic defects [49]. As a result, the coatings created using laser cladding technology not only contain the excellent qualities of HEA materials but also can establish a strong link with the substrate material, strengthening the material's ability to resist corrosion. The fundamental idea behind the two types of synchronous powder feeding and pre-powdering used in laser cladding technology is depicted in Figure 3a.

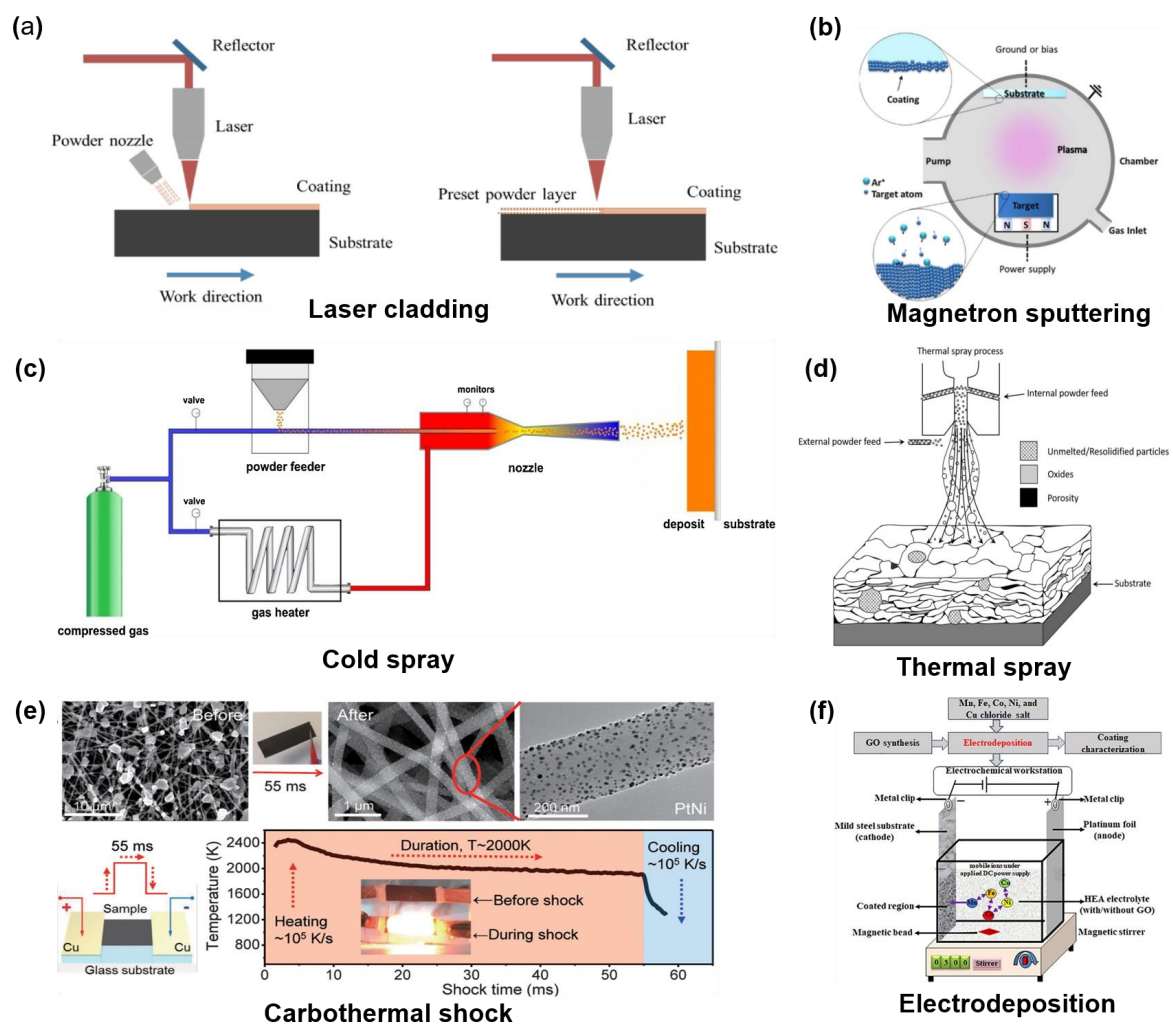


Figure 3. The fabrication methods of HEA coatings. (a) Laser cladding [50]. Copyright 2018 Elsevier. (b) Magnetron sputtering [51]. Copyright 2016 Elsevier. (c) Cold spray [52]. Copyright 2018 Elsevier. (d) Thermal spray [53]. (e) Carbothermal shock [14]. Copyright 2018 The American Association for the Advancement of Science. (f) Electrodeposition [54]. Copyright 2022 Elsevier.

The selection of parameters for the preparation process of high-entropy coatings is equally as crucial as the nature of the material itself in determining how well it performs. In general, the preparation process for laser-clad high-entropy coatings can be optimized by adjusting the laser power, laser scanning speed, laser beam size, powder feeding speed, pre-placement powder thickness, nozzle angle, and filling distance, all of which affect the coating's microstructure, surface morphology, and service life. HEA coatings prepared by laser cladding may produce defects including non-uniform composition, porosity, cracks, inclusions, incomplete melting, presence of residual stresses, and weak bonding between coating and substrate; therefore, how to optimize laser cladding process parameters is one of the popular research directions, among which scanning speed and laser power are significant factors in determining the coating performance.

Scanning speed: Qiu et al. [55] prepared AlCrFeCuCo high-entropy coatings by laser cladding that primarily has the phase compositions FCC and BCC. The corrosion resistance study discovered that, within a certain range, the alloy's corrosion resistance tended to enhance first, and then weaken (Figure 4), which was caused by the decrease in laser energy absorbed by the molten layer material with the increase in scanning speed. The higher cooling rate makes the surface of the molten layer smooth and dense. This helps to improve the coating's corrosion resistance, but if the scanning speed is excessively high, it is easy to

form a rough and porous surface of the molten layer, which leads to the deterioration of the corrosion resistance of the coating.

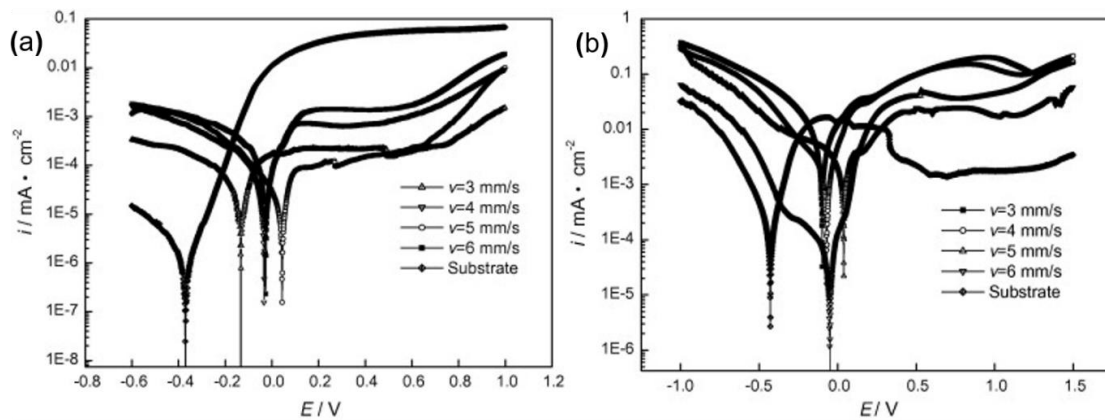


Figure 4. Potentiodynamic polarization curves for AlCrFeCoCu high-entropy alloys [55]. (a) In 1 mol/L NaCl solution. (b) In 0.5 mol/L H₂SO₄ solution. Copyright 2013 Elsevier.

Laser power: Shu et al. [56] prepared CoCrBFeNiSi high-entropy coatings on H13 steel using different laser powers (233 W, 476 W, 583 W, and 700 W). The molten layer consisted mainly of dendritic crystals at the bottom and amorphous crystals at the top. The laser power influences the dilution rate and the actual cooling rate by modulating the heat input, thus changing the amorphous content of the coating, with the highest amorphous content of the samples at a laser power of 476 W, followed by samples prepared at 233 W, 583 W, and 700 W. Figure 5 shows the EIS plots and polarization curves of the substrate and coating of the samples under the conditions of 3.5 wt.% NaCl solution and 1 mol/L HCl solution. The reduction in the amorphous content was found to significantly decrease the impedance spectral radius and helped to increase the coating's corrosion potential after being compared to the amorphous content at different laser powers. Therefore, it can be judged that the coating's ability to resist corrosion is primarily influenced by its amorphous content.

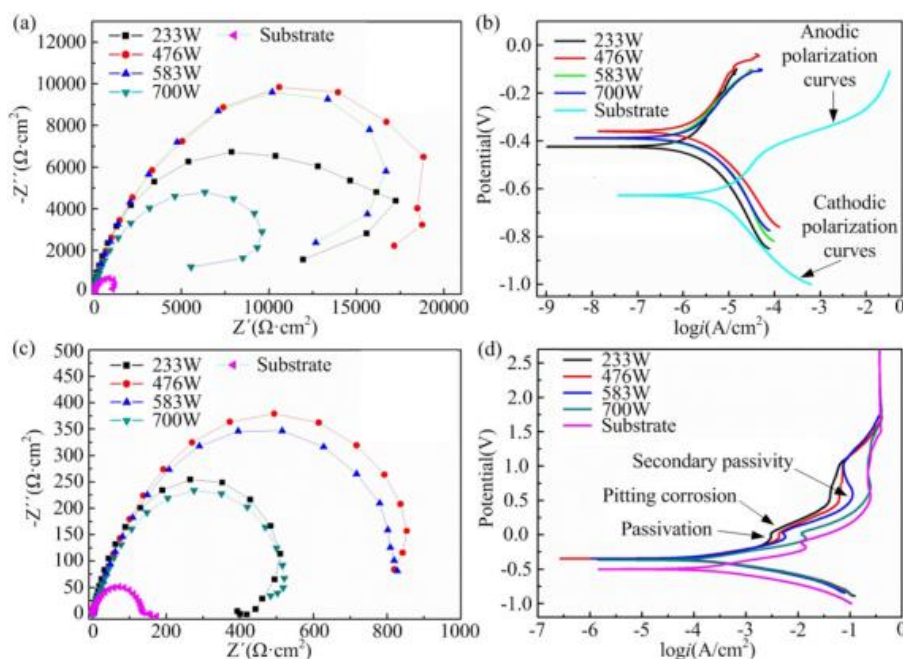


Figure 5. The electrochemistry test result of the substrate and coatings [56]. (a) EIS diagram in 3.5 wt.% NaCl solution, (b) polarization curves in 3.5 wt.% NaCl solution, (c) EIS diagram in 1 mol/L HCl solution, (d) polarization curves in 1 mol/L HCl solution. Copyright 2018 Elsevier.

2.2.2. Magnetron Sputtering

First, the electric field inside the cavity is used to ionize Ar atoms, producing a large amount of high-energy Ar⁺ and electrons, and then the surface of the prefabricated target is bombarded with high energy under the action of the electric field. After energy exchange, the metal on the surface of the target is sputtered from the surface of the prefabricated target in an atomic or ionic state, and the internal magnetic field influences the atoms to move directionally and then creates the HEA coating. Figure 3b shows the principle of magnetron sputtering. The coating prepared by magnetron sputtering technology has the technical advantages of a smooth and dense surface, uniform composition, high flexibility, and stable process. However, it also has some drawbacks: only nano- or micron-level films can be formed, the bond between the coating and the substrate is weak, and the preparation process is complicated.

Process parameters during magnetron sputtering, such as substrate temperature, sputtering power, bias voltage, target base distance, and power supply type, may affect the microstructure and properties of the coatings prepared by magnetron sputtering. Sometimes deposition temperature and sputtering power play a more significant role in enhancing coating quality and corrosion resistance.

Deposition temperature: With different deposition temperatures (100 °C, 200 °C, and 300 °C), He et al. [57] prepared TiVZrCrAl HEA coatings on Zr-4 alloy using RF magnetron sputtering. Due to the higher temperature's benefits on atom diffusion and migration, surface morphologies coarsen with deposition temperature increases (Figure 6). When the deposition temperature was 300 °C, the coating had a strong bonding with the substrate, according to research on how deposition temperature affected the microstructure and mechanical properties of the coatings. Additionally, in static pure water, the corrosion performance of the coatings applied at 300 °C was studied. Based on the results, a high temperature encouraged the production of AlVO₄, which then enhanced the Zr-4 substrate's corrosion resistance by preventing the dissolution of Al in the form of AlOOH.

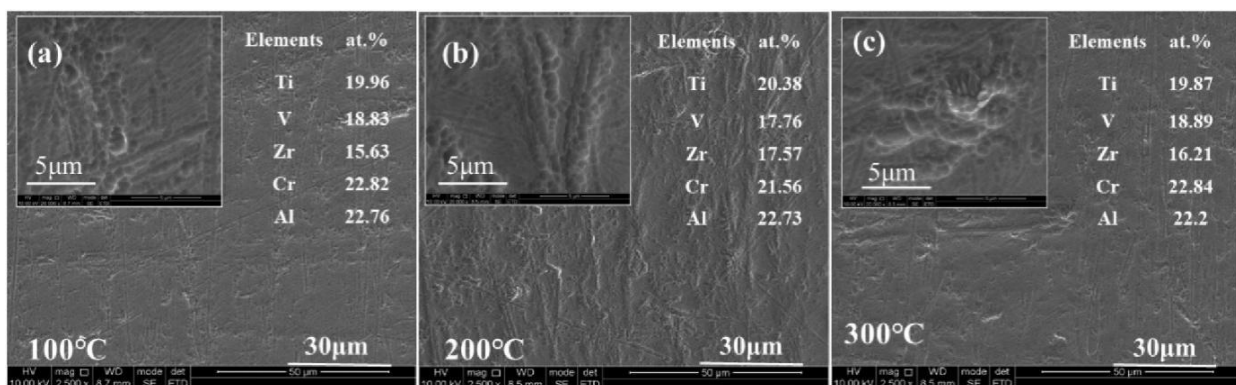


Figure 6. SEM images and elemental compositions of the TiVZrCrAl coatings' surface at different deposition temperatures [57]: (a) 100 °C, (b) 200 °C, (c) 300 °C. Copyright 2022 Elsevier.

With different substrate temperatures (ranging from 25 °C to 700 °C), Song et al. [58] prepared TaNbHfZr films with various microstructures and discovered that the atomic diffusion ability significantly increased with the increase in deposition temperature, causing the phase structure of the film to change from amorphous to nanocrystalline BCC phase. This is because the capacity of the sputtered atoms to diffuse to the substrate surface increases significantly as the substrate temperature rises, inducing grain growth while also eliminating the hole boundary caused by the amorphous state. It is significant to mention that the amorphous content has a massive effect on the coating's ability to resist corrosion [56] since the absence of grain boundaries in the amorphous structure makes it more resistant to corrosion than the crystalline structure. Therefore, a prudent choice of deposition temperature can ensure the coating's corrosion resistance.

Sputtering power: At three different RF powers (200 W, 250 W, and 300 W), HEA films of AlCoCrCu_{0.5}FeNi were deposited by Khan [59]. As shown in Figure 7, the films prepared at zero RF power have FCC+BCC solid solution structure, and when the RF power is increased, the films' crystallinity rises. Additionally, the oxide formation is affected by the RF power, which may also have an impact on the corrosion resistance of the coating.

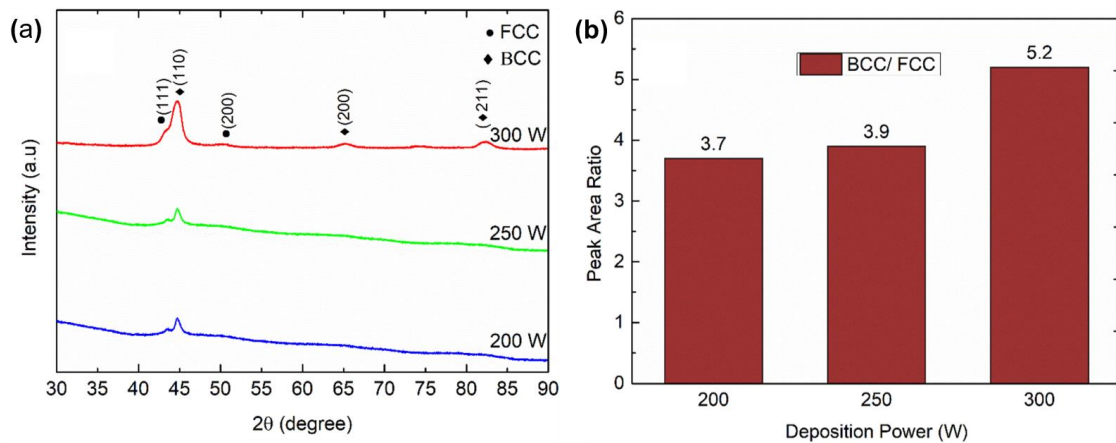


Figure 7. Crystal structure of film under different RF powers. (a) XRD plots, (b) peak area ratios of BCC and FCC contents of AlCoCrCu_{0.5} FeNi films grown at three different RF powers [59]. Copyright 2020 Elsevier.

For preparing high-entropy coatings/thin films, laser cladding and magnetron sputtering are the two most commonly used techniques. However, both techniques have some drawbacks, such as high equipment costs for laser cladding, difficulty in tuning process parameters, and the tendency to produce coatings with cracks. Magnetron sputtering can produce coatings/films with thicknesses limited to the nano- or micron-scale, the preparation process is more complicated, and often the bonding strength between the coating and the substrate is not high enough. Therefore, one of the current research hotspots is the quest for a preparation process that better satisfies the needs of high-entropy coatings/thin films.

2.2.3. Thermal Spray Technology

The thermal spray technique (Figure 3d) has drawn the interest of researchers. The thermal spray process is susceptible to impurities such as oxides and changes in tissue structure, and the quality of HEA coatings produced by thermal spray technology is inferior compared to that of the other two technologies. Nevertheless, thermal spray technology is ideal for mass production due to its benefits, such as a controllable process, lower cost, and minimal impact on the substrate. Thermal spray technology can be further divided into plasma spray, supersonic flame spray, high-speed arc spray, cold spray, and other technologies. Among them, the application of the cold spray method can avoid the phase change and oxidation defects caused by heat input, prepare a thick coating with dense organization, and improve the corrosion resistance of the coating. For the first time, Anupam et al. [60] prepared an AlCoCrFeNi HEA coating on the surface of a Ni-based alloy by the cold spray technique (Figure 3c). At 1100 °C, an oxide layer formed on the surface of this coating could protect the substrate for 25 h, significantly enhancing the coating's oxidation resistance and corrosion resistance.

2.2.4. Electrodeposition Technology

By electrodeposition technology (Figure 3f), graphite oxide (GO) was compounded in AlCrFeCoNiCu HEA composite coating. Aliyu et al. [61] deposited the coating on a mild steel substrate, which was tested for corrosion resistance in a 3.5 wt.% NaCl aqueous solution, and the results showed that the corrosion resistance gradually increased with the addition of GO content in the coating. The reason is that the addition of GO promotes the

homogeneity of microstructure and composition, thus avoiding local corrosion due to current coupling caused by elemental segregation, improving the corrosion resistance of the HEA-GO composite coating; Cr promotes the formation of metal oxide films on the coating surface, thus reducing ion diffusion and improving the corrosion resistance of the coating [62].

2.3. Potential New Technologies

High-entropy coatings have various excellent properties that traditional coating materials do not have, but the preparation processes for high-entropy coatings are still in the laboratory research stage and cannot be used for large-scale production applications. Therefore, some potential preparation processes are proposed in this paper, aiming to provide ideas for the development of new high-entropy coating preparation processes to solve some problems of existing preparation processes.

2.3.1. Low-Temperature Plasma Surface Modification Technology

The generated plasma can be divided into high-temperature plasma (from 10^6 to 10^8 K) and low-temperature plasma (room temperature 3×10^4 K), depending on the gas temperature of the ionizer. Low-temperature plasma can be further divided into hot plasma (from 3×10^3 to 3×10^4 K), non-thermal plasma (from 200 to 1000 K), and cold plasma (room temperature 200 °C). Among them is thermal plasma spray technology, which is a kind of thermal spray technology. Wang et al. [63] prepared $(\text{CoCrFeNi})_{95}\text{Nb}_5$ HEA coating on Q235 steel substrate by plasma spray technique, and found that due to the high cooling rate of the plasma spray technique and the good bonding of the coating to the substrate, elemental segregation occurred in the dendrites and interdendrites of the coating, and the Cr and Nb enriched in the interdendritic phase acted as the anode for the corrosion to occur preferentially. The $(\text{CoCrFeNi})_{95}\text{Nb}_5$ coating prepared by plasma spray technology can significantly improve the corrosion resistance of Q235 steel substrates. Low-temperature plasma may also be used for material surface modification, such as reducing the wettability of the material coating surface, preparing a superhydrophobic surface, waterproofing, self-cleaning, and anti-corrosion of acid and alkali liquid. Alternatively, low-temperature plasma can be used to make the material substrate surface rougher, which expands the contact area between the substrate and the coating, thus enhancing the bonding strength of the substrate and the coating. It can be said that low-temperature plasma surface modification technology is a highly potent tool for pre-treatment, post-treatment, and even the whole preparation process of HEA coatings. The stability of the non-equilibrium plasma and the produced volume limitations are still challenges that need to be resolved. It has enormous potential for the preparation of HEA coatings.

2.3.2. Carbothermal Shock Ultra-Fast Cooling Synthesis Technology

The addition of expensive elements is one of the main factors making industrial mass production of HEAs challenging. Although HEA coatings can be regarded as a promising solution, the cost of the coating itself cannot be ignored, especially in industrial mass production, where controlling the cost of the HEA coating is crucial. Yao et al. [14] achieved a homogeneous mixture of inexpensive alloy elements that are otherwise incompatible, resulting in a HEA with uniform size and distribution nanoparticles with a composition of up to eight elements using a straightforward two-step carbothermal shock (CTS) method, in which a metal precursor salt is attached to oxidized carbon fiber, and then heated to ~ 2000 K for 55 ms at a rate of up to 100,000 K per second and then cooled (Figure 3e). In addition, a programmable heating and quenching mode (PHQ) was developed [64,65] that enables fast switching of the reactant temperature between about 600 K and 2000 K, thus allowing the chemical reaction to proceed far from equilibrium. In addition to carbon thermal shock technology, this intelligent management of process parameters also applies to laser cladding, magnetron sputtering, and thermal spray technologies, which may assist in boosting production scale, productivity, and product quality. Moreover, the short heating time and fast cooling are very ideal for coating preparation, because the

short heating means acting on the surface of the substrate material, while the fast cooling helps to ensure the uniform and dense structure of the coating is generated on the entire substrate surface, resulting in HEA coatings with excellent performance. Additionally, the basic research on the elemental composition and various process parameters on the microstructure and material properties may be accelerated by using the thermal shock ultra-fast cooling synthesis technique to quickly prepare small samples. It is crucial to note that compared with the traditional constant temperature heating method, PHQ reduces energy consumption by up to 80% and achieves the effect of energy saving and emission reduction in a real sense by using clean electrical energy for heating, which is conducive to reducing the production cost and is expected to be put into large-scale industrial use.

Based on the pertinent research discussed above, Figure 8 provides a general overview of the various fabrication methods and a comparison of five factors: time, temperature, performance, cost, and applicability. The comparative research reveals that while laser cladding and magnetron sputtering have better overall performances, their costs are greater and their processes are more uncontrollable, making it challenging to accomplish industrial mass production. The properties of the prepared coatings need to be improved, despite the low cost, ease of use, and industrial production potential of thermal spraying technology. Electrochemical deposition and low-temperature plasma technologies can be used as post-treatment processes for coatings, such as chemical plating on the surface of the coating or modification of the coating surface by low-temperature plasma to improve the performance of the coating. CTS has the characteristics of ultra-fast heating and cooling, which is conducive to the preparation of a uniform structure of the coating and can reduce the use of expensive metals, greatly reducing the cost, and has great potential.

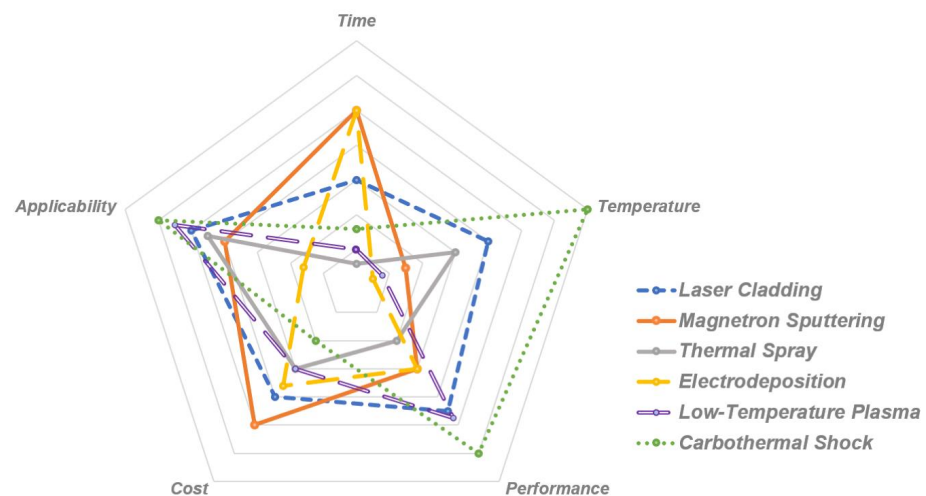


Figure 8. Summarize and compare different fabrication methods based on time–temperature–performance–cost–applicability.

In addition to the above-mentioned preparation techniques, there are also laser surface alloying [66], plasma cladding [67], powder metallurgy [68], and electro-spark deposition [69], etc. However, all of these techniques have some drawbacks and need to be improved or combined with other processes or techniques to produce HEA coatings with excellent performance. Among them, post-treatment has a significant role in improving the surface quality and microstructure of the coating.

2.4. Post-Treatment Technologies

The current preparation processes, such as laser cladding, magnetron sputtering, thermal spraying, etc., inevitably lead to heterogeneous coatings in the thickness direction and forming direction, including the structure, chemical composition, coating properties, etc., due to the parameters of the preparation process, the physical and chemical properties

of the materials used, and the gas environment. The high-temperature preparation process under a gaseous environment is also likely to produce pores, cracks, and gaps, resulting in a decrease in the denseness of the coating and worse surface quality, which affects the corrosion resistance of the coating. In severe cases, it may lead to poor bonding between the coating and the substrate, making the coating peel off from the substrate. Therefore, the reasonable use of different post-treatment processes or the development of more efficient, energy-saving, and environmentally friendly post-treatment methods can effectively control the microstructure and surface quality of the coating, thus improving the performance of the coating.

2.4.1. Annealing Treatment

Although a series of high-temperature preparation processes, such as laser cladding, have great advantages in preparing dense coatings, their ultra-fast cooling process can easily lead to various problems, such as residual internal stress, phase separation, elemental segregation, lattice distortion, etc. A suitable heat treatment process, especially annealing, can play a significant role in improving such problems and enhancing the corrosion resistance of coatings. Zhu et al. [70] performed water quenching as a post-treatment process by holding the coating at 1000 °C for 2 h. The original microstructure in the CoCrFeNi HEA coating was completely transformed from columnar grains to equiaxed grains (Figure 9a). In addition, during high-temperature annealing, equiaxed grains are prone to nucleation and growth and undergo recrystallization processes, thus eliminating residual strain. More critically, the cell structure and elemental segregation are also completely removed, as shown in Figure 9b–f. The uniform element distribution of the coating results in higher corrosion potential and lower corrosion current density, enhancing the corrosion resistance of the coating. This indicates that the annealing treatment can effectively enhance the uniformity of the coating and alleviate the disadvantages of laser cladding.

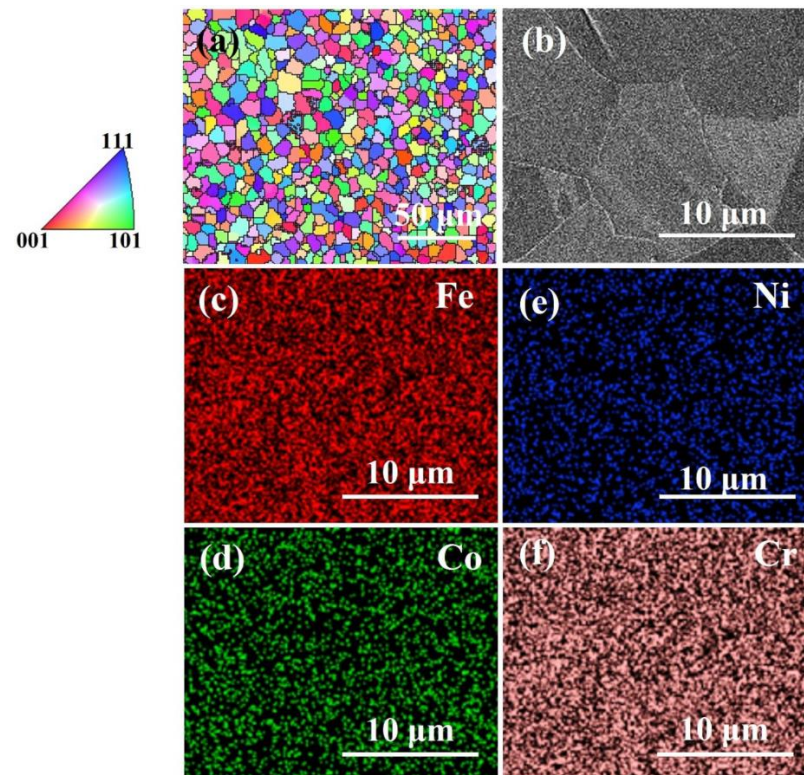


Figure 9. (a) EBSD IPF map of the 1000 °C annealed CoCrFeNi coating. (b) A typical SEM micrograph. (c–f) corresponding EDS mapping results of the 1000 °C annealed CoCrFeNi coating [70]. Copyright 2022 Elsevier.

2.4.2. Friction Stir Processing

Friction stir processing (FSP) is often considered an effective post-treatment for modifying the microstructure of HEAs. Especially widely used in coatings prepared by techniques such as laser cladding, FSP leads to strong plastic deformation, material mixing, and thermal exposure, resulting in significant refinement, densification, and homogeneity of the microstructure in the processed area [71]. This has a significant effect on improving the surface quality of the coating and improving properties such as corrosion and friction resistance.

Kumar et al. [72] used FSP to post-treat Al_{0.1}CoCrFeNi; the FSP-treated grains were significantly refined, and the average grain size was $\sim 14 \pm 10 \mu\text{m}$ at an HAGB cut-off angle of 15° . A friction stir processed Fe_{38.5}Mn₂₀Co₂₀Cr₁₅Si₅Cu_{1.5} (Cu-HEA) was prepared by Nene et al. [73], which obtained fine grains and a stable γ phase. Cu was more dissolved in the matrix due to the strong plastic deformation and mass friction heat during the FSP; minimization of Cu partitioning within the γ matrix would make the alloy more corrosion-resistant thermodynamically and kinetically. Figure 10 shows the effect of grain size on the corrosion resistance of HEA coatings; the anodic region showing a steeper slope than the FSP condition in Figure 10a(a₁) means that the anodic region in the as-cast condition corrodes more rapidly, and higher anodic means as-FSP conditions have the tendency to passivate. This corresponds to the previous discussion that a more uniform structure, finer grains, and passivation films improve the corrosion resistance of coatings.

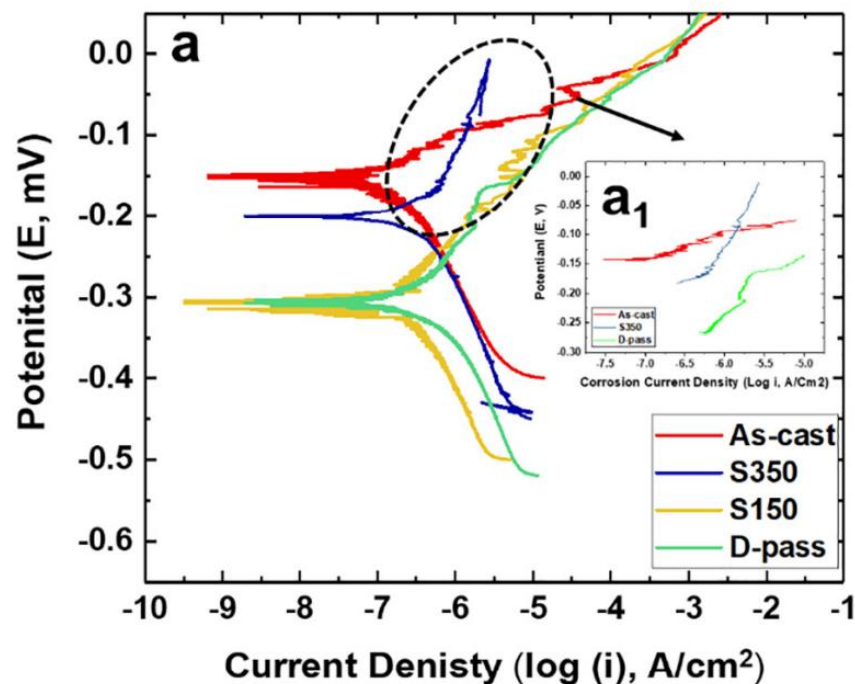


Figure 10. Corrosion behavior of Cu-HEA: (a) Tafel polarization plots for as-cast and as-FSP conditions in 3.5 wt% NaCl solution. (a₁) Local amplification. [73]. Copyright 2019 Elsevier.

2.4.3. Laser Re-Melting

Laser re-melting (LR) is similar to the laser cladding process, but no cladding powder is added to the re-melting process. LR allows the formation of a melt pool on the coating surface and supports ultra-fast cooling rates of up to 10^5 K/s . This facilitates the elimination of internal defects in the coating, the expansion of the solid solution limit, the refinement of microstructure, the elimination of elemental segregation, the improvement in surface quality, and the preparation of HEA coatings with excellent properties; thus, laser melting and LR can be used in combination for more efficient preparation of high-performance HEA coatings [74]. Chong et al. [75] prepared AlCoCrFeNi HEA coatings using a combination of high-speed laser cladding (HLC) and LR. The coatings prepared by HLC had liquid

phase separation (LPS) zones, which exhibited Ni-poor, low-hardness, and easy-flaking characteristics and had a great impact on the corrosion and wear resistance of the coatings. The LR eliminates several LPS zones in the coating with fine equiaxed grains and provides a large driving force for grain boundary segregation due to more high-angle grain boundaries caused by LR. The Cr content at the grain boundaries becomes higher, resulting in a significant improvement in the corrosion resistance of the LR coating.

The above are several common post-treatment processes. Other processes, such as ultrasonic impact [76] and ultrasonic surface rolling treatment [77], etc., also have good effects on the microstructure and surface quality of the coating. Most of the post-treatment processes focus on refining grain size, reducing elemental segregation, reducing porosity, cracks, and improving densities to improve coatings' wear resistance and corrosion resistance. In addition to the fabrication method and post-treatment process, the elemental composition of the HEA coating is also critical.

3. Effect of Elements on Corrosion Resistance of HEA Coatings

The structure of a material affects its properties, which are related to the thermodynamic entropy, enthalpy, and electronegativity of the elements that make up the alloy [78], electronegativity [79], atomic radius [80], etc. To promote the formation of solid solution in the alloy, the general principle of alloy solid solution formation follows Hume-Rothery rules, which means that alloy elements with high mixed entropy, similar electronegativity, and a small difference in atomic radius should be selected. Atomic size difference (δ) and mixing enthalpy (ΔH_{mix}) were combined by Zhang et al. [81] to predict HEAs. As shown in Figure 11, a HEA solid solution phase will be obtained at $\delta \leq 6.6\%$ and $-11.6 \text{ kJ}\cdot\text{mol}^{-1} \leq \Delta H_{\text{mix}} \leq 3.2 \text{ kJ}\cdot\text{mol}^{-1}$.

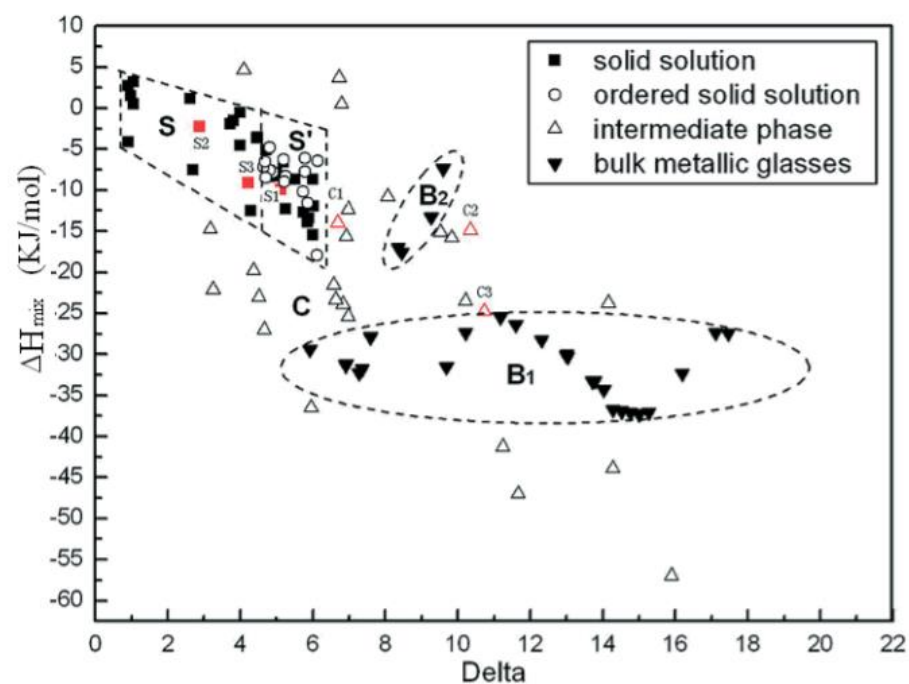


Figure 11. Relationship between atomic size difference (Delta) and mixing enthalpy (ΔH_{mix}) for MHAs and typical multicomponent bulk metallic glasses [81]. (“solid solution” indicates the alloy contains only solid solution, “ordered solid solution” indicates minor ordered solid solution precipitate besides solid solution, and “intermediate phase” indicates there is precipitation of intermediate phases like intermetallics in HEAs. Red sign represents the alloys designed to verify the phase formation rules for multicomponent HEAs. Copyright 2008, Wiley.

A detailed comparison of the corrosion behavior of HEAs with traditional alloys (stainless steels, Al alloys, Ti alloys, Cu alloys, and Ni alloys) in 3.5 wt.% NaCl solution

(Figure 12a) and 0.5 M H₂SO₄ solution (Figure 12b) is shown in Figure 12, where E_{pit} (breakdown potential) is used as an index to evaluate the pitting resistance of the material, and i_{corr} (corrosion current density) is a kinetic parameter of the corrosion behavior of the material, which is related to the corrosion rate. The HEAs are located in the lower right part of Figure 12a,b, indicating that the local and overall corrosion resistance of HEAs is comparable to, or even better than, that of conventional corrosion-resistant alloys in common salt or acidic solutions. Additionally, HEA coatings can be improved by post-treatment to improve their corrosion resistance, so HEA coatings are considered to be a material with huge advantages in aqueous corrosive environments.

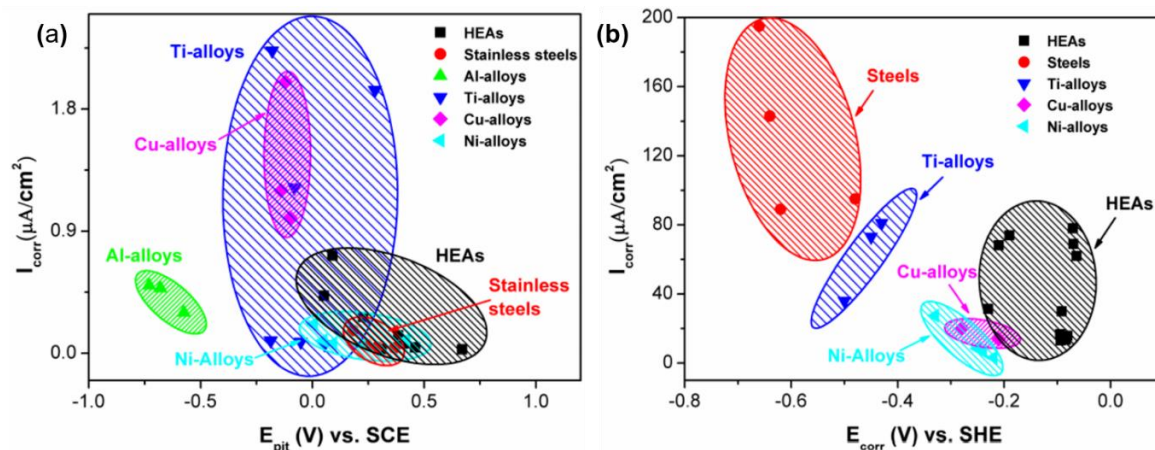


Figure 12. A comparison of the corrosion current density (i_{corr}) and pitting potential (E_{pit}) between HEAs and other materials at room temperature. (a) In the 3.5 wt.% NaCl solution. (b) In the 0.5 M H₂SO₄ solution [82].

Cr, Al, Co, Ni, Fe, Cu, Ti, Zr, Nb, Mo, W, V, and other metal elements are commonly used in HEA coatings. Among them, Cr, Co, Ni, Cu, Ti, Nb, Mo, etc., have excellent corrosion resistance and will form a homogeneous and dense passive film on the surface when exposed to corrosion, which is tightly bonded with the matrix of the alloy and can play a significant role in inhibiting corrosion, but the content of easy passive elements may not be the more, the better. When the content of an easy passive element in the coating is too high, it will lead to a heterogeneous composition and structure of the coating, resulting in component segregation and affecting the corrosion resistance of the coating. Consequently, the kind and content of elements play an important role in the corrosion resistance of the coating.

The influence of Si, Mn, and Mo additions on the melt-coated CoCrCuFeNi high-entropy coating on the surface of Q235 steel was researched by Zhang et al. [49]. The phase structure of the coating was a simple FCC solid solution in the absence of Si, Mn, and Mo additions, primarily composed of columnar and equiaxed grains with uniform distribution of alloying elements and low component segregation. However, the bond between the coating and the substrate is not tight enough, which indicates that the quality of the coating is unsatisfactory. The addition of Si, Mn, and Mo significantly improves the performance of the coating. Despite a slight increase in composition deviation and the transformation of the microstructure to dendrites, the CoCrCuFeNi high-entropy coating maintains a respectable level of corrosion resistance and overall performance.

With laser cladding, Ye et al. [83] prepared the Al_xCoCrCuFeNi high-entropy coating successfully on 45# steel, which showed FCC and BCC structures with dendritic and interdendritic organizations in the microstructure without any voids or cracks, and although it had the same structure as the cast sample, the degree of Cu segregation between dendrites was much lower than that of the cast prepared sample. This is because the dendrite growth direction is primarily influenced by the heat flow density of the melt pool: there is a large temperature gradient at the bottom of the coating, where the columnar dendrites tend to grow perpendicular to the substrate surface, and in the top region, the heat flow density is

mainly controlled by the heat flow density of the melt pool. The corrosion resistance of the coating is influenced by the uniform element distribution, and the $\text{Al}_x\text{CoCrCuFeNi}$ coating shows better corrosion resistance than 314 L stainless steel in 0.05 M HCl. This indicates that whether the element distribution is uniform is one of the important indicators of the corrosion resistance of the coating, and excessive elemental segregation may lead to the occurrence of partial corrosion phenomena. It shows that ensuring the uniformity of each part of the coating is the key factor for the corrosion resistance of the coating.

$\text{Al}_2\text{CrFeCoCuTiNi}_x$ high-entropy coatings consisting of a melting zone, a bonding zone, and a heat-affected zone were prepared by Qiu et al. [84] on Q235 steel employing a laser cladding technique. There is a good metallurgical bond between the melt layer and the substrate, and the melt zone consists mainly of axial crystals, nanocrystals, and fine white crystals with a simple phase structure (FCC and BCC structure). The corrosion behavior was studied, and it was found that the coating has good corrosion resistance in 1 M NaOH solution and 3.5 wt.% NaCl solution, and that the corrosion resistance improves and then decreases with the increase in Ni content. This is because Ni has strong corrosion resistance, and the higher the Ni addition, the easier it is for the coating to prepare a dense passive film. However, since the atomic radius of Ni is relatively small and the HEA has the nature of lattice distortion, excessive Ni addition will lead to serious lattice distortion and affect the uniformity of the microstructure of the alloy, which in turn affects the corrosion resistance. Additionally, by increasing the Ti content, Qiu et al. [85] found that the corrosion resistance of $\text{Al}_2\text{CrFeCoCuNiTi}_x$ high-entropy coatings in 0.5 M HNO_3 solutions was enhanced, because higher Ti content could promote the formation of Ti_2O_3 and TiO_2 passive films.

Due to the content of passive elements Cr and Ni, FeCoCrNi-based HEA coatings usually have excellent corrosion resistance, and in general, the addition of Al and Ti has a better effect on improving the mechanical properties (density and plasticity) and wear resistance of HEA coatings. It has been shown that the passive film has the best corrosion resistance when the molar ratio of Ti in FeCoCrNi-based HEA coatings is 1.0 [86–88]; the optimal molar ratio of Ti for HEA coatings with different compositions still needs to be investigated. To study the corrosion characteristics of HEA coatings in-depth, specialized tests can be performed for different forms of corrosion, including atmospheric corrosion, pitting corrosion, crevice corrosion, intergranular corrosion, hydrogen cracking, and stress corrosion cracking [89].

Table 2 summarizes the electrochemical corrosion parameters that some current studies on the effects of several common alloy elements on the corrosion resistance of HEA coatings have obtained. The majority of research focuses on how the addition of certain passivating materials affects the corrosion resistance of coatings. Generally, the high-entropy alloy coating has a substantially better level of corrosion resistance than the metal substrate. Within a particular range, the presence of these passivating elements contributes to the coating's corrosion resistance, and most of them accomplish this by influencing the passivating film's forming characteristics (such as uniformity, density, etc.). However, it is possible to produce substantial lattice distortion, non-uniform composition, and other defects, which might reduce the coating's corrosion resistance when the content of passivating elements (such as Ni) is too high. Additionally, the segregation of Cu may damage the homogeneity of Cr, Co, and Ni, thus worsening passive film formation [90]. The influence of Al on the corrosion resistance of the coating is still controversial; Shi et al. [91] found that the increase in Al content will have a negative impact on the protective ability of the passive film; the passive film's Cr oxide/hydroxide ratio decreases with a rise in Al content. However, pertinent studies indicate that the addition of Al can prevent dendritic segregation of Cu, and encourage a homogenous distribution of Cu between dendrites and interdendrites [92]. This demonstrates a further problem; despite how the synergistic effect of multiple elements may greatly enhance the performance of the coating, most studies today only search for a single element's influence, and it is unclear how multiple elements interact to produce

a synergistic effect, leading to a bottleneck in the element design of HEAs, which is not conducive to fully exploiting the cocktail effect and designing high-performance HEAs.

Table 2. Electrochemical corrosion parameters of HEA coatings with different alloy elements.

Element	Coatings	Substrates	Solution	E_{corr} (V)	i_{corr} (A/cm ²)	Reference
Cr	AlCoCr _{0.5} FeNi	45# steel	0.1 M HCl	−0.403	7.19×10^{-4}	[93]
	AlCoCr _{1.5} FeNi			−0.293	1.18×10^{-5}	[93]
	AlCoCr _{2.0} FeNi			−0.373	2.47×10^{-4}	[93]
Cr	AlCr _{0.5} NiCu _{0.5} Mo	Q235 steel	3.5 wt.% NaCl	−1.056	2.86×10^{-4}	[94]
	AlCr _{1.5} NiCu _{0.5} Mo			−0.989	3.88×10^{-4}	[94]
	AlCr _{2.0} NiCu _{0.5} Mo			−0.949	2.23×10^{-4}	[94]
Al	CoCrFeNiTi	AISI1045 steel	3.5 wt.% NaCl	−0.738	5.60×10^{-6}	[95]
	CoCrFeNiTiAl _{0.5}			−0.577	9.13×10^{-7}	[95]
	CoCrFeNiTiAl			−0.679	5.43×10^{-6}	[95]
Al+Cr	[Al-(FeCoNi) ₁₂]Cr ₃	904 L stainless steel	35 wt.% H ₃ PO ₄ and 40 wt.% H ₂ SO ₄	−0.367	3.67×10^{-5}	[96]
	[Al-(FeCoNi) ₁₂]AlCr ₂			−0.339	4.99×10^{-6}	[96]
	[Al-(FeCoNi) ₁₂]Al _{1.5} Cr _{1.5}			−0.317	1.49×10^{-6}	[96]
Ni	FeCoCrAlCuNi _{0.5}	cp Cu	3.5 wt.% NaCl	−0.270	7.84×10^{-7}	[97]
	FeCoCrAlCuNi			−0.250	3.63×10^{-7}	[97]
	FeCoCrAlCuNi _{1.5}			−0.210	7.48×10^{-7}	[97]
Cu	Al _{0.8} CrFeCoNiCu _{0.5}	Al alloy	0.1 M H ₂ SO ₄	−0.384	2.56×10^{-5}	[90]
	Al _{0.8} CrFeCoNiCu _{0.75}			−0.462	4.28×10^{-5}	[90]
	Al _{0.8} CrFeCoNiCu			−0.502	4.93×10^{-5}	[90]
Ti	CoCrFeNiTi _{0.1}	Q235 steel	3.5 wt.% NaCl	−1.180	5.64×10^{-6}	[98]
	CoCrFeNiTi _{0.3}			−1.160	4.23×10^{-6}	[98]
	CoCrFeNiTi _{0.5}			−1.130	3.81×10^{-6}	[98]
Ti	CoCr _{2.5} FeNi ₂ Ti _{0.5}	Q235 steel	saturated salt solution	−0.578	4.89×10^{-5}	[88]
	CoCr _{2.5} FeNi ₂ Ti			−0.228	1.39×10^{-5}	[88]
	CoCr _{2.5} FeNi ₂ Ti _{1.5}			−0.263	2.28×10^{-5}	[88]
Mo	Ni _{1.5} CrFeTi ₂ B _{0.5}	904 L stainless steel	simulated saturated saline–water mud	−0.587	6.43×10^{-6}	[99]
	Ni _{1.5} CrFeTi ₂ B _{0.5} Mo _{0.25}			−0.461	5.21×10^{-6}	[99]
	Ni _{1.5} CrFeTi ₂ B _{0.5} Mo _{0.5}			−0.437	1.78×10^{-6}	[99]
	Ni _{1.5} CrFeTi ₂ B _{0.5} Mo _{0.75}			−0.384	6.89×10^{-6}	[99]

Based on the present research data, it is roughly estimated that the molar ratio of Cr in FeCoCrNi-based HEA should be <2.0, and the molar ratio of Ni should be <1.0. To better understand the effect of adding two or more other different alloying elements on the corrosion resistance of coatings, the corrosion behavior of CoCrFeNi-based HEAs (including CoCr_{y-x}FeNi_x, Al_xCoCr_{y-x}FeNi, CoCrFeNi_xTi_{y-x}, Al_{y-x}CoCrFeNiCu_x, etc.) can be systematically investigated using rigorous electrochemistry and more advanced surface characterization.

4. Conclusions and Future Work

This paper reviews the definition, advantages, and properties of HEAs and summarizes some advantages of HEA coatings in solving the problems of high-cost and complex processes of bulk HEAs. It is worth noting that the preparation of HEA coating materials is usually based on the study of the properties of the current research system of bulk HEAs, while it is difficult to ensure that the current research system of bulk HEAs applies to coating/film materials due to their thermodynamic high-entropy effect, structural lattice distortion effect, kinetic hysteresis diffusion effect, or performance cocktail effect. Analysis of the recent research progress on HEA coatings leads to the main conclusions as follows.

- The structural characteristics and advantages of HEAs are very suitable for the preparation of HEA coatings with corrosion resistance, friction and wear proper-

ties, high-temperature resistance, and high-strength hardness to meet the material performance requirements needed for human beings' in-depth explorations in the fields of aerospace, marine shipping, and new energy. In particular, HEA coatings with excellent corrosion resistance and anti-scouring properties have great potential for applications in fields such as deep-sea corrosion and high-temperature erosion;

- The main existing preparation techniques for high-entropy coatings include laser cladding, magnetron sputtering, thermal spray, and electrodeposition. In addition to the elemental composition of the coating material itself, the variation of the preparation process parameters will also influence the microstructure, tissue morphology, phase composition, and surface properties of the coating. For example, scanning speed and laser power for laser cladding, deposition temperature, and sputtering power for magnetron sputtering, etc. Laser cladding and magnetron sputtering are currently the most widely used techniques for preparing and improving high-entropy coatings, but both methods are difficult to achieve large-scale use for, while thermal spray technology is widely applicable and is expected to be the future industrial production technology for high-entropy coatings;
- The corrosion resistance of the high-entropy coating is closely related to the elemental composition of the material itself, especially for Cr, Co, Ni, Cu, Ti, Nb, Mo, and other elements, which are the main elements for the formation of the passive film and all have excellent corrosion resistance. However, passive elements should not be used in excess, because they may tend to lead to component segregation and intensify the lattice distortion effect of the high-entropy coating, which will have negative effects on the corrosion resistance of the coating.

In recent years, HEA shapes such as bulk HEAs, HEA coatings, and HEA powders have drawn a lot of attention and widespread interest in scientific research and potential industrial applications, but the knowledge of HEA materials and related coatings is still very limited. As shown in Figure 13, the following development trends and possible future applications for HEA coatings are therefore proposed in light of the current problems with HEA coating design, preparation, and other aspects.

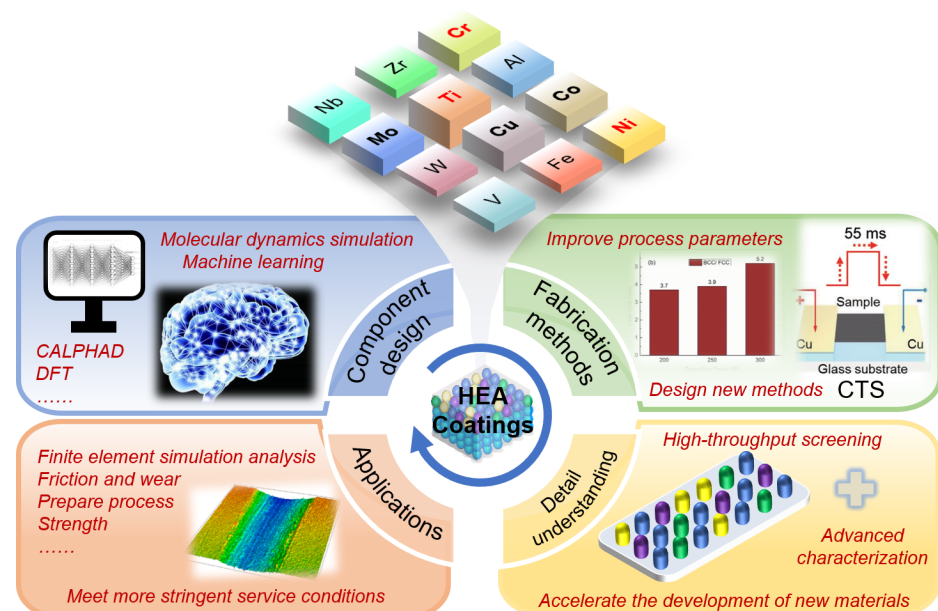


Figure 13. The schematic diagram of the future development of HEA coatings based on composition–process–understanding–application, especially in the following three aspects: high-throughput screening and multi-scale simulation accelerated material development, systematic research on the design, development and basic theory of new HEA and HEA coatings, optimization of the preparation process of HEA coatings, and design of new processes.

- Systematic research on the design, development, and basic theory of new HEAs and HEA coatings: the current properties and performance of HEA coatings mainly refer to the relevant research on HEA bulks. However, due to the wide range of elemental composition and elemental content uncertainty, the composition design of HEA coatings cannot be rigidly applied according to the research on HEA bulks. Additionally, most current research focuses on how a single element affects an alloy system's properties, and there is little research on the synergistic mechanism of multiple elements, which is unfavorable for giving full play to the cocktail effect of HEAs and designing the best performance of HEA coatings. Therefore, further research is needed on the basic theory of HEA coatings, including the system design of the elemental composition, and the effects of the interaction and coordination mechanism between multiple elements on the microstructure and properties of coatings.
- Optimization of the preparation process of HEA coatings and design of new processes: the performance of microstructure, phase composition, and surface properties of HEA coatings depends on the composition and process, and a reasonable process design can prepare HEA coatings with excellent performance, but there are still some drawbacks in the preparation process used today. For example, porosity, cracks, and dilution are common problems in the laser cladding process, but they can be optimized by regulating the parameters such as scanning rate and laser power, and other parameters can be optimized. Therefore, the preparation process can be optimized to greatly improve the material's corrosion resistance and keep costs under control. Moreover, by combining the current processes with low-temperature plasma surface modification technology or thermal shock ultra-fast cooling synthesis technology, fresh ideas and solutions to alleviate the defects of the current preparation process can be gained, which can complement each other and further accelerate the development of new HEA coating materials and deepen the research on the material structure and properties.
- High-throughput experiments and multi-scale simulations accelerate material development: one of the characteristics of HEA materials is the diverse selection and combination of elements, which means that the traditional experimental approach-oriented "trial-and-error" research and design model is no longer applicable to the development of HEA coating materials. Computational material science involves all aspects of materials; there are corresponding material calculation methods at different spatial scales, and with the rapid development of characterization technology, property testing technology, and computer technology (artificial intelligence, machine learning, etc. [100–102]), a large amount of data can be obtained in a short time, and the relationship between elemental composition, process parameters, and properties can be analyzed to filter out the suitable elemental composition ratio and process parameters to accelerate the development of new HEA coatings. Zhu et al. [103] have developed a full-process machine chemist, which can search and read the relevant literature, summarize and analyze, perform diversified and customized tasks, perform intelligent experimental operations and search for global-optimal solutions, and complete all the process steps of conventional experiments. The speed of material development is greatly accelerated, which is the initial realization of intelligent, digital, and automated material design. Therefore, in the future, researchers would be expected to flexibly apply advanced computer technology to support the development of new HEA coatings with excellent properties, improve the efficiency of materials development, and reduce costs.
- Demand-oriented design of HEA coatings with the required properties and finite element simulation analysis to promote the development of HEA coatings for industrial applications: to realize the industrial application of HEA coatings, it is necessary to first ensure the rationality of composition design, excellent performance, etc., followed by the controllability of cost, utilization of resources, etc., and finally the feasibility and controllability of the preparation process. By simulating the coating preparation process through finite element analysis, we can judge the feasibility and scientificity

of the preparation process to improve the preparation process parameters more efficiently, and simulate and verify whether the service performance of the coating meets the requirements according to the service conditions of the coating.

The service conditions of coatings are often complex, and corrosion resistance cannot be considered alone. For example, in a high-temperature and high-pressure environment, it should also have high-temperature resistance to prevent the coating from falling off, and in a friction environment, it should also have friction and wear resistance, and different environments should have different physical, chemical, and mechanical properties. Due to its unique characteristics, HEA is more advantageous in preparing coatings with multiple properties, making applying HEA coatings in various fields very promising.

Author Contributions: Writing—original draft preparation, C.L.; writing—review and editing, C.L. and Y.Y.; project administration, Y.Y. All authors have read and agreed to the published version of the manuscript.

Funding: This research received no funding.

Institutional Review Board Statement: Not applicable.

Informed Consent Statement: Not applicable.

Data Availability Statement: Not applicable.

Conflicts of Interest: The authors declare no conflict of interest.

References

1. Yeh, J.W.; Chen, S.K.; Lin, S.J.; Gan, J.Y.; Chin, T.S.; Shun, T.T.; Tsau, C.H.; Chang, S.Y. Nanostructured high-entropy alloys with multiple principal elements: Novel alloy design concepts and outcomes. *Adv. Eng. Mater.* **2004**, *6*, 299–303. [[CrossRef](#)]
2. Chen, T.K.; Shun, T.T.; Yeh, J.W.; Wong, M.S. Nanostructured nitride films of multi-element high-entropy alloys by reactive DC sputtering. *Surf. Coat. Technol.* **2004**, *188*, 193–200. [[CrossRef](#)]
3. Cantor, B.; Chang, I.T.H.; Knight, P.; Vincent, A.J.B. Microstructural development in equiatomic multicomponent alloys. *Mater. Sci. Eng. A Struct. Mater. Prop. Microstruct. Process.* **2004**, *375*, 213–218. [[CrossRef](#)]
4. Yao, Y.; Dong, Q.; Brozina, A.; Luo, J.; Miao, J.; Chi, M.; Wang, C.; Kevrekidis, I.G.; Ren, Z.J.; Greeley, J.; et al. High-entropy nanoparticles: Synthesis-structure-property relationships and data-driven discovery. *Science* **2022**, *376*, eabn3103. [[CrossRef](#)] [[PubMed](#)]
5. Ye, Y.F.; Wang, Q.; Lu, J.; Liu, C.T.; Yang, Y. High-entropy alloy: Challenges and prospects. *Mater. Today* **2016**, *19*, 349–362. [[CrossRef](#)]
6. Miracle, D.B.; Senkov, O.N. A critical review of high entropy alloys and related concepts. *Acta Mater.* **2017**, *122*, 448–511. [[CrossRef](#)]
7. Zhang, Y.; Zuo, T.T.; Tang, Z.; Gao, M.C.; Dahmen, K.A.; Liaw, P.K.; Lu, Z.P. Microstructures and properties of high-entropy alloys. *Prog. Mater. Sci.* **2014**, *61*, 1–93. [[CrossRef](#)]
8. Sathiyamoorthi, P.; Kim, H.S. High-entropy alloys with heterogeneous microstructure: Processing and mechanical properties. *Prog. Mater. Sci.* **2022**, *123*, 100709. [[CrossRef](#)]
9. Shi, P.; Ren, W.; Zheng, T.; Ren, Z.; Hou, X.; Peng, J.; Hu, P.; Gao, Y.; Zhong, Y.; Liaw, P.K. Enhanced strength-ductility synergy in ultrafine-grained eutectic high-entropy alloys by inheriting microstructural lamellae. *Nat. Commun.* **2019**, *10*, 489. [[CrossRef](#)]
10. Lei, Z.; Liu, X.; Wu, Y.; Wang, H.; Jiang, S.; Wang, S.; Hui, X.; Wu, Y.; Gault, B.; Kontis, P.; et al. Enhanced strength and ductility in a high-entropy alloy via ordered oxygen complexes. *Nature* **2018**, *563*, 546–550. [[CrossRef](#)]
11. Guo, R.; Yu, L.; Liu, Z.; Pan, J.; Yao, Y.; Liu, L. Enthalpy induced phase partition toward hierarchical, nanostructured high-entropy alloys. *Nano Res.* **2022**, *15*, 4893–4901. [[CrossRef](#)]
12. Yu, L.; Zeng, K.; Li, C.; Lin, X.; Liu, H.; Shi, W.; Qiu, H.-J.; Yuan, Y.; Yao, Y. High-entropy alloy catalysts: From bulk to nano toward highly efficient carbon and nitrogen catalysis. *Carbon Energy* **2022**, *4*, 731–761. [[CrossRef](#)]
13. Wang, X.; Guo, W.; Fu, Y. High-entropy alloys: Emerging materials for advanced functional applications. *J. Mater. Chem. A* **2021**, *9*, 663–701. [[CrossRef](#)]
14. Yao, Y.; Huang, Z.; Xie, P.; Lacey, S.D.; Jacob, R.J.; Xie, H.; Chen, F.; Nie, A.; Pu, T.; Rehwoldt, M.; et al. Carbothermal shock synthesis of high-entropy-alloy nanoparticles. *Science* **2018**, *359*, 1489–1494. [[CrossRef](#)]
15. Zhang, Y.; Zuo, T.; Cheng, Y.; Liaw, P.K. High-entropy Alloys with High Saturation Magnetization, Electrical Resistivity, and Malleability. *Sci. Rep.* **2013**, *3*, 1455. [[CrossRef](#)] [[PubMed](#)]
16. Shi, W.; Liu, H.; Li, Z.; Li, C.; Zhou, J.; Yuan, Y.; Jiang, F.; Fu, K.; Yao, Y. High-entropy alloy stabilized and activated Pt clusters for highly efficient electrocatalysis. *SusMat* **2022**, *2*, 186–196. [[CrossRef](#)]
17. Wang, Z.; Ge, H.; Liu, S.; Li, G.; Gao, X. High-Entropy Alloys to Activate the Sulfur Cathode for Lithium-Sulfur Batteries. *Energy Environ. Mater.* **2022**, *Online ahead of print*. [[CrossRef](#)]
18. Li, J.; Huang, Y.; Meng, X.; Xie, Y. A Review on High Entropy Alloys Coatings: Fabrication Processes and Property Assessment. *Adv. Eng. Mater.* **2019**, *21*, 1900343. [[CrossRef](#)]

19. Yan, X.; Zou, Y.; Zhang, Y. Properties and processing technologies of high-entropy alloys. *Mater. Futures* **2022**, *1*, 22002. [[CrossRef](#)]
20. Santodonato, L.J.; Zhang, Y.; Feygenson, M.; Parish, C.M.; Gao, M.C.; Weber, R.J.K.; Neufeind, J.C.; Tang, Z.; Liaw, P.K. Deviation from high-entropy configurations in the atomic distributions of a multi-principal-element Alloys. *Nat. Commun.* **2015**, *6*, 5964. [[CrossRef](#)]
21. Zhang, X.; Liu, L.; Yao, K.; Duan, K.; Wu, F.; Zhao, R.; Zhang, Y.; Shang, J.; Chen, M. The phase composition characteristics of AlCoCrFeNi high entropy alloy heat-treated by simple normalizing treatment and its effects on mechanical properties. *J. Alloys Compd.* **2022**, *926*, 166896. [[CrossRef](#)]
22. Popescu, A.-M.J.; Branzoi, F.; Burada, M.; Atkinson, I.; Constantin, I.; Moreno, J.C.; Miculescu, F.; Mitrica, D.; Badea, I.-C.; Oлару, M.T.; et al. Influence of Heat Treatment on the Corrosion Behavior of Electrodeposited CoCrFeMnNi High-Entropy Alloy Thin Films. *Coatings* **2022**, *12*, 1108. [[CrossRef](#)]
23. Akhlaghi, P.; Amirjan, M.; Parvin, N. The effect of processing parameters and heat-treatment on the microstructure and mechanical properties of PM CoCrFeMnNiTi0.1 high-entropy Alloys. *Mater. Chem. Phys.* **2021**, *257*, 123722. [[CrossRef](#)]
24. Xian, X.; Zhong, Z.-H.; Lin, L.-J.; Zhu, Z.-X.; Chen, C.; Wu, Y.-C. Tailoring strength and ductility of high-entropy CrMnFeCoNi alloy by adding Al. *Rare Met.* **2022**, *41*, 1015–1021. [[CrossRef](#)]
25. Gao, J.; Jin, Y.; Fan, Y.; Xu, D.; Meng, L.; Wang, C.; Yu, Y.; Zhang, D.; Wang, F. Fabricating antibacterial CoCrCuFeNi high-entropy alloy via selective laser melting and in-situ alloying. *J. Mater. Sci. Technol.* **2022**, *102*, 159–165. [[CrossRef](#)]
26. Li, D.; Li, C.; Feng, T.; Zhang, Y.; Sha, G.; Lewandowski, J.J.; Liaw, P.K.; Zhang, Y. High-entropy Al0.3CoCrFeNi alloy fibers with high tensile strength and ductility at ambient and cryogenic temperatures. *Acta Mater.* **2017**, *123*, 285–294. [[CrossRef](#)]
27. Shen, Q.; Kong, X.; Chen, X. Fabrication of bulk Al-Co-Cr-Fe-Ni high-entropy alloy using combined cable wire arc additive manufacturing (CCW-AAM): Microstructure and mechanical properties. *J. Mater. Sci. Technol.* **2021**, *74*, 136–142. [[CrossRef](#)]
28. Srivastava, M.; Jadhav, M.; Chethan; Chakradhar, R.P.S.; Muniprakash, M.; Singh, S. Synthesis and properties of high velocity oxy-fuel sprayed FeCoCrNi2Al high entropy alloy coating. *Surf. Coat. Technol.* **2019**, *378*, 124950. [[CrossRef](#)]
29. Cheng, H.; Pan, Z.; Fu, Y.; Wang, X.; Wei, Y.; Luo, H.; Li, X. Review-Corrosion-Resistant High-Entropy Alloy Coatings: A Review. *J. Electrochem. Soc.* **2021**, *168*, 111502. [[CrossRef](#)]
30. Joseph, J.; Haghdadi, N.; Shamlaye, K.; Hodgson, P.; Barnett, M.; Fabijanic, D. The sliding wear behaviour of CoCrFeMnNi and AlxCoCrFeNi high entropy alloys at elevated temperatures. *Wear* **2019**, *428*, 32–44. [[CrossRef](#)]
31. Sheikh, S.; Shafeie, S.; Hu, Q.; Ahlstrom, J.; Persson, C.; Vesely, J.; Zyka, J.; Klement, U.; Guo, S. Alloy design for intrinsically ductile refractory high-entropy alloys. *J. Appl. Phys.* **2016**, *120*, 164902. [[CrossRef](#)]
32. He, Z.; Guo, Y.; Sun, L.; Yan, H.-L.; Guan, X.; Jiang, S.; Shen, Y.; Yin, W.; Zhao, X.; Li, Z.; et al. Interstitial-driven local chemical order enables ultrastrong face-centered cubic multicomponent alloys. *Acta Mater.* **2022**, *243*, 118495. [[CrossRef](#)]
33. Zhong, C.; Liu, F.; Wu, Y.; Le, J.; Liu, L.; He, M.; Zhu, J.; Hu, W. Protective diffusion coatings on magnesium alloys: A review of recent developments. *J. Alloys Compd.* **2012**, *520*, 11–21. [[CrossRef](#)]
34. Hu, R.-G.; Zhang, S.; Bu, J.-F.; Lin, C.-J.; Song, G.-L. Recent progress in corrosion protection of magnesium alloys by organic coatings. *Prog. Org. Coat.* **2012**, *73*, 129–141. [[CrossRef](#)]
35. Ye, K.; Li, Z. Toward Ceramic Anticorrosion Coatings: A Review. *Corrosion* **2020**, *76*, 595–916. [[CrossRef](#)]
36. Zhang, P.; Li, Z.; Liu, H.; Zhang, Y.; Li, H.; Shi, C.; Liu, P.; Yan, D. Recent progress on the microstructure and properties of high entropy alloy coatings prepared by laser processing technology: A review. *J. Manuf. Process.* **2022**, *76*, 397–411. [[CrossRef](#)]
37. Zhao, S.; Liu, C.; Yang, J.; Zhang, W.; He, L.; Zhang, R.; Yang, H.; Wang, J.; Long, J.; Chang, H. Mechanical and high-temperature corrosion properties of AlTiCrNiTa high entropy alloy coating prepared by magnetron sputtering for accident-tolerant fuel cladding. *Surf. Coat. Technol.* **2021**, *417*, 127228. [[CrossRef](#)]
38. Meghwal, A.; Anupam, A.; Murty, B.S.; Berndt, C.C.; Kottada, R.S.; Ang, A.S.M. Thermal Spray High-Entropy Alloy Coatings: A Review. *J. Therm. Spray Technol.* **2020**, *29*, 857–893. [[CrossRef](#)]
39. Cui, H.; Jiang, D. Research Progress of High-Entropy Alloy Coatings. *Acta Metall. Sin.* **2022**, *58*, 17–27. [[CrossRef](#)]
40. Cantor, B. Multicomponent high-entropy Cantor alloys. *Prog. Mater. Sci.* **2021**, *120*, 100754. [[CrossRef](#)]
41. Bhardwaj, V.; Zhou, Q.; Zhang, F.; Han, W.; Du, Y.; Hua, K.; Wang, H. Effect of Al addition on the microstructure, mechanical and wear properties of TiZrNbHf refractory high entropy alloys. *Tribol. Int.* **2021**, *160*, 107031. [[CrossRef](#)]
42. Sharma, A. High Entropy Alloy Coatings and Technology. *Coatings* **2021**, *11*, 372. [[CrossRef](#)]
43. Cheng, J.; Sun, B.; Ge, Y.; Hu, X.; Zhang, L.; Liang, X.; Zhang, X. Effect of B/Si ratio on structure and properties of high-entropy glassy Fe25Co25Ni25(BxSi1-x)(25) coating prepared by laser cladding. *Surf. Coat. Technol.* **2020**, *402*, 126320. [[CrossRef](#)]
44. Braic, V.; Balaceanu, M.; Braic, M.; Vladescu, A.; Panseri, S.; Russo, A. Characterization of multi-principal-element (TiZrNbHfTa)N and (TiZrNbHfTa)C coatings for biomedical applications. *J. Mech. Behav. Biomed. Mater.* **2012**, *10*, 197–205. [[CrossRef](#)]
45. Sarkar, A.; Wang, Q.; Schiele, A.; Chellali, M.R.; Bhattacharya, S.S.; Wang, D.; Brezesinski, T.; Hahn, H.; Velasco, L.; Breitung, B. High-Entropy Oxides: Fundamental Aspects and Electrochemical Properties. *Adv. Mater.* **2019**, *31*, e1806236. [[CrossRef](#)] [[PubMed](#)]
46. Guo, Y.-X.; Liu, Q.-B.; Shang, X.-J. In situ TiN-reinforced CoCr(2)FeNiTi(0.5)high-entropy alloy composite coating fabricated by laser cladding. *Rare Met.* **2020**, *39*, 1190–1195. [[CrossRef](#)]
47. Jiang, P.F.; Zhang, C.H.; Zhang, S.; Zhang, J.B.; Chen, J.; Liu, Y. Fabrication and wear behavior of TiC reinforced FeCoCrAlCu-based high entropy alloy coatings by laser surface alloying. *Mater. Chem. Phys.* **2020**, *255*, 123571. [[CrossRef](#)]
48. Aliyu, A.; Srivastava, C. Microstructure-corrosion property correlation in electrodeposited AlCrFeCoNiCu high entropy alloys-graphene oxide composite coatings. *Thin Solid Films* **2019**, *686*, 137434. [[CrossRef](#)]

49. Zhang, H.; Pan, Y.; He, Y.Z. Synthesis and characterization of FeCoNiCrCu high-entropy alloy coating by laser cladding. *Mater. Des.* **2011**, *32*, 1910–1915. [[CrossRef](#)]
50. Yan, X.H.; Li, J.S.; Zhang, W.R.; Zhang, Y. A brief review of high-entropy films. *Mater. Chem. Phys.* **2018**, *210*, 12–19. [[CrossRef](#)]
51. Calderon Velasco, S.; Cavaleiro, A.; Carvalho, S. Functional properties of ceramic-Ag nanocomposite coatings produced by magnetron sputtering. *Prog. Mater. Sci.* **2016**, *84*, 158–191. [[CrossRef](#)]
52. Yin, S.; Cavaliere, P.; Aldwell, B.; Jenkins, R.; Liao, H.; Li, W.; Lupoi, R. Cold spray additive manufacturing and repair: Fundamentals and applications. *Addit. Manuf.* **2018**, *21*, 628–650. [[CrossRef](#)]
53. Tejero-Martin, D.; Rezvani Rad, M.; McDonald, A.; Hussain, T. Beyond Traditional Coatings: A Review on Thermal-Sprayed Functional and Smart Coatings. *J. Therm. Spray Technol.* **2019**, *28*, 598–644. [[CrossRef](#)]
54. Aliyu, A.; Srivastava, C. Phase constitution, surface chemistry and corrosion behavior of electrodeposited MnFeCoNiCu high entropy alloy-graphene oxide composite coatings. *Surf. Coat. Technol.* **2022**, *429*, 127943. [[CrossRef](#)]
55. Qiu, X.-W.; Zhang, Y.-P.; He, L.; Liu, C.-g. Microstructure and corrosion resistance of AlCrFeCuCo high entropy Alloys. *J. Alloys Compd.* **2013**, *549*, 195–199. [[CrossRef](#)]
56. Shu, F.; Zhang, B.; Liu, T.; Sui, S.; Liu, Y.; He, P.; Liu, B.; Xu, B. Effects of laser power on microstructure and properties of laser cladded CoCrBFeNiSi high-entropy alloy amorphous coatings. *Surf. Coat. Technol.* **2019**, *358*, 667–675. [[CrossRef](#)]
57. He, L.; Liu, C.; Zhao, S.; Shu, C.; Yang, J.; Liu, H.; Zhang, W.; Lin, J.; Long, J.; Chang, H. Microstructure, mechanical and corrosion properties of high hardness TiVZrCrAl HEA coatings prepared by magnetron sputtering. *Surf. Coat. Technol.* **2022**, *441*, 128532. [[CrossRef](#)]
58. Song, B.; Li, Y.; Cong, Z.; Li, Y.; Song, Z.; Chen, J. Effects of deposition temperature on the nanomechanical properties of refractory high entropy TaNbHfZr films. *J. Alloys Compd.* **2019**, *797*, 1025–1030. [[CrossRef](#)]
59. Khan, N.A.; Akhavan, B.; Zhou, C.; Zhou, H.; Chang, L.; Wang, Y.; Liu, Y.; Fu, L.; Bilek, M.M.; Liu, Z. RF magnetron sputtered AlCoCrCu0.5FeNi high entropy alloy (HEA) thin films with tuned microstructure and chemical composition. *J. Alloys Compd.* **2020**, *836*, 155348. [[CrossRef](#)]
60. Anupam, A.; Kumar, S.; Chavan, N.M.; Murty, B.S.; Kottada, R.S. First report on cold-sprayed AlCoCrFeNi high-entropy alloy and its isothermal oxidation. *J. Mater. Res.* **2019**, *34*, 796–806. [[CrossRef](#)]
61. Aliyu, A.; Rekha, M.Y.; Srivastava, C. Microstructure–electrochemical property correlation in electrodeposited CuFeNiCoCr high-entropy alloy-graphene oxide composite coatings. *Philos. Mag.* **2019**, *99*, 718–735. [[CrossRef](#)]
62. Aliyu, A.; Srivastava, C. Corrosion behavior and protective film constitution of AlNiCoFeCu and AlCrNiCoFeCu high entropy alloy coatings. *Surf. Interfaces* **2021**, *27*, 101481. [[CrossRef](#)]
63. Wang, W.; Qi, W.; Xie, L.; Yang, X.; Li, J.; Zhang, Y. Microstructure and Corrosion Behavior of (CoCrFeNi)₉₅Nb-5 High-Entropy Alloy Coating Fabricated by Plasma Spraying. *Materials* **2019**, *12*, 694. [[CrossRef](#)] [[PubMed](#)]
64. Dong, Q.; Yao, Y.; Cheng, S.; Alexopoulos, K.; Gao, J.; Srinivas, S.; Wang, Y.; Pei, Y.; Zheng, C.; Brozena, A.H.; et al. Programmable heating and quenching for efficient thermochemical synthesis. *Nature* **2022**, *605*, 470–476. [[CrossRef](#)]
65. Li, S.; Zhang, H.; Ruan, H.; Cheng, Z.; Yao, Y.; Zhuge, F.; Zhai, T. Programmable Nucleation and Growth of Ultrathin Tellurium Nanowires via a Pulsed Physical Vapor Deposition Design. *Adv. Funct. Mater.* **2022**, *Online ahead of print*. [[CrossRef](#)]
66. Wu, C.L.; Xu, T.Z.; Wang, Z.Y.; Zhang, C.H.; Zhang, S.; Ni, C.L.; Zhang, D.X. Laser surface alloying of FeCoCrAlNiTi high entropy alloy composite coatings reinforced with TiC on 304 stainless steel to enhance wear behavior. *Ceram. Int.* **2022**, *48*, 20690–20698. [[CrossRef](#)]
67. Wang, M.; Lu, Y.; Zhang, G.; Cui, H.; Xu, D.; Wei, N.; Li, T. A novel high-entropy alloy composite coating with core-shell structures prepared by plasma cladding. *Vacuum* **2021**, *184*, 109905. [[CrossRef](#)]
68. Eissmann, N.; Kloeden, B.; Weissgaerber, T.; Kieback, B. High-entropy alloy CoCrFeMnNi produced by powder metallurgy. *Powder Metall.* **2017**, *60*, 184–197. [[CrossRef](#)]
69. Geambazu, L.E.; Voiculescu, I.; Manea, C.A.; Bololoi, R.V. Economic Efficiency of High-Entropy Alloy Corrosion-Resistant Coatings Designed for Geothermal Turbine Blades: A Case Study. *Appl. Sci.* **2022**, *12*, 7196. [[CrossRef](#)]
70. Zhu, Q.; Liu, Y.; Zhang, C. Laser cladding of CoCrFeNi high-entropy alloy coatings: Compositional homogeneity towards improved corrosion resistance. *Mater. Lett.* **2022**, *318*, 132133. [[CrossRef](#)]
71. Ma, Z.Y. Friction Stir Processing Technology: A Review. *Metall. Mater. Trans. A* **2008**, *39*, 642–658. [[CrossRef](#)]
72. Kumar, N.; Komarasamy, M.; Nelaturu, P.; Tang, Z.; Liaw, P.K.; Mishra, R.S. Friction Stir Processing of a High Entropy Alloy Al_{0.1}CoCrFeNi. *JOM* **2015**, *67*, 1007–1013. [[CrossRef](#)]
73. Nene, S.S.; Frank, M.; Liu, K.; Sinha, S.; Mishra, R.S.; McWilliams, B.A.; Cho, K.C. Corrosion-resistant high entropy alloy with high strength and ductility. *Scr. Mater.* **2019**, *166*, 168–172. [[CrossRef](#)]
74. Karimi, J.; Antonov, M.; Kollo, L.; Prashanth, K.G. Role of laser remelting and heat treatment in mechanical and tribological properties of selective laser melted Ti6Al4V Alloys. *J. Alloys Compd.* **2022**, *897*, 163207. [[CrossRef](#)]
75. Chong, Z.; Sun, Y.; Cheng, W.; Huang, L.; Han, C.; Ma, X.; Meng, A. Laser remelting induces grain refinement and properties enhancement in high-speed laser cladding AlCoCrFeNi high-entropy alloy coatings. *Intermetallics* **2022**, *150*, 107686. [[CrossRef](#)]
76. Zhang, S.; Han, B.; Li, M.; Hu, C.; Zhang, Q.; Liu, X.; Wang, Y. Investigation on microstructure and properties of laser cladded AlCoCrCuFeNi high entropy alloy coating by ultrasonic impact treatment. *Intermetallics* **2021**, *128*, 107017. [[CrossRef](#)]
77. Cui, Z.; Qin, Z.; Dong, P.; Mi, Y.; Gong, D.; Li, W. Microstructure and corrosion properties of FeCoNiCrMn high entropy alloy coatings prepared by high speed laser cladding and ultrasonic surface mechanical rolling treatment. *Mater. Lett.* **2020**, *259*, 126769. [[CrossRef](#)]
78. Otto, F.; Yang, Y.; Bei, H.; George, E.P. Relative effects of enthalpy and entropy on the phase stability of equiatomic high-entropy alloys. *Acta Mater.* **2013**, *61*, 2628–2638. [[CrossRef](#)]

79. Leong, Z.; Huang, Y.; Goodall, R.; Todd, I. Electronegativity and enthalpy of mixing biplots for High Entropy Alloy solid solution prediction. *Mater. Chem. Phys.* **2018**, *210*, 259–268. [[CrossRef](#)]
80. Wang, Z.; Qiu, W.; Yang, Y.; Liu, C.T. Atomic-size and lattice-distortion effects in newly developed high-entropy alloys with multiple principal elements. *Intermetallics* **2015**, *64*, 63–69. [[CrossRef](#)]
81. Zhang, Y.; Zhou, Y.J.; Lin, J.P.; Chen, G.L.; Liaw, P.K. Solid-solution phase formation rules for multi-component alloys. *Adv. Eng. Mater.* **2008**, *10*, 534–538. [[CrossRef](#)]
82. Shi, Y.; Yang, B.; Liaw, P.K. Corrosion-Resistant High-Entropy Alloys: A Review. *Metals* **2017**, *7*, 43. [[CrossRef](#)]
83. Ye, X.; Ma, M.; Cao, Y.; Liu, W.; Ye, X.; Gu, Y. The Property Research on High-entropy Alloy Al_xFeCoNiCuCr Coating by Laser Cladding. *Phys. Procedia* **2011**, *12*, 303–312. [[CrossRef](#)]
84. Qiu, X.-W.; Liu, C.-G. Microstructure and properties of Al₂CrFeCoCuTiNi_x high-entropy alloys prepared by laser cladding. *J. Alloys Compd.* **2013**, *553*, 216–220. [[CrossRef](#)]
85. Qiu, X.W.; Zhang, Y.P.; Liu, C.G. Effect of Ti content on structure and properties of Al₂CrFeNiCoCuTi_x high-entropy alloy coatings. *J. Alloys Compd.* **2014**, *585*, 282–286. [[CrossRef](#)]
86. Wu, C.L.; Zhang, S.; Zhang, C.H.; Zhang, H.; Dong, S.Y. Phase evolution and cavitation erosion-corrosion behavior of FeCoCrAlNiTi_x high entropy alloy coatings on 304 stainless steel by laser surface alloying. *J. Alloys Compd.* **2017**, *698*, 761–770. [[CrossRef](#)]
87. Liu, J.; Liu, H.; Chen, P.; Hao, J. Microstructural characterization and corrosion behaviour of AlCoCrFeNiTi_x high-entropy alloy coatings fabricated by laser cladding. *Surf. Coat. Technol.* **2019**, *361*, 63–74. [[CrossRef](#)]
88. Gu, Z.; Xi, S.; Sun, C. Microstructure and properties of laser cladding and CoCr(2.5)FeNi(2)Ti_x high-entropy alloy composite coatings. *J. Alloys Compd.* **2020**, *819*, 152986. [[CrossRef](#)]
89. Qiu, Y.; Thomas, S.; Gibson, M.A.; Fraser, H.L.; Biribilis, N. Corrosion of high entropy alloys. *NPJ Mater. Degrad.* **2017**, *1*, 15. [[CrossRef](#)]
90. Jiang, Y.Q.; Li, J.; Juan, Y.F.; Lu, Z.J.; Jia, W.L. Evolution in microstructure and corrosion behavior of AlCoCr_xFeNi high-entropy alloy coatings fabricated by laser cladding. *J. Alloys Compd.* **2019**, *775*, 1–14. [[CrossRef](#)]
91. Liu, X.-Q.; Zhang, Y.-X.; Wang, X.-R.; Wang, Z.-Q.; He, P. Microstructure and corrosion properties of AlCr_xNiCu0.5Mo (x = 0, 0.5, 1.0, 1.5, 2.0) high entropy alloy coatings on Q235 steel by electrospark—Computer numerical control deposition. *Mater. Lett.* **2021**, *292*, 129642. [[CrossRef](#)]
92. Xu, Y.; Li, Z.; Liu, J.; Chen, Y.; Zhang, F.; Wu, L.; Hao, J.; Liu, L. Microstructure Evolution and Properties of Laser Cladding CoCrFeNiTiAl_x High-Entropy Alloy Coatings. *Coatings* **2020**, *10*, 373. [[CrossRef](#)]
93. Lan, H.; Liu, Q. Design of Al-(FeCoNi)₁₂ Al_xCr_{3-x} HEAs based on cluster-plus-gluce-atom model and its coating fabricated by laser cladding. *Intermetallics* **2020**, *126*, 106941. [[CrossRef](#)]
94. Wu, C.L.; Zhang, S.; Zhang, C.H.; Zhang, H.; Dong, S.Y. Phase evolution and properties in laser surface alloying of FeCoCrAlCuNi_x high-entropy alloy on copper substrate. *Surf. Coat. Technol.* **2017**, *315*, 368–376. [[CrossRef](#)]
95. Li, Y.; Shi, Y.; Olugbade, E. Microstructure, mechanical, and corrosion resistance properties of Al_{0.8}CrFeCoNiCu_x high-entropy alloy coatings on aluminum by laser cladding. *Mater. Res. Express* **2020**, *7*, 26504. [[CrossRef](#)]
96. Wang, X.; Liu, Q.; Huang, Y.; Xie, L.; Xu, Q.; Zhao, T. Effect of Ti Content on the Microstructure and Corrosion Resistance of CoCrFeNiTi_x High Entropy Alloys Prepared by Laser Cladding. *Materials* **2020**, *13*, 2209. [[CrossRef](#)] [[PubMed](#)]
97. Gu, Z.; Peng, W.; Guo, W.; Zhang, Y.; Hou, J.; He, Q.; Zhao, K.; Xi, S. Design and characterization on microstructure evolution and properties of laser-cladding Ni_{1.5}CrFeTi₂B_{0.5}Mo_x high-entropy alloy coatings. *Surf. Coat. Technol.* **2021**, *408*, 126793. [[CrossRef](#)]
98. Shi, Y.; Yang, B.; Rack, P.D.; Guo, S.; Liaw, P.K.; Zhao, Y. High-throughput synthesis and corrosion behavior of sputter-deposited nanocrystalline Al_x(CoCrFeNi)_{100-x} combinatorial high-entropy alloys. *Mater. Des.* **2020**, *195*, 109018. [[CrossRef](#)]
99. Li, Y.; Shi, Y. Microhardness, wear resistance, and corrosion resistance of Al_xCrFeCoNiCu high-entropy alloy coatings on aluminum by laser cladding. *Opt. Laser Technol.* **2021**, *134*, 106632. [[CrossRef](#)]
100. Hart, G.L.W.; Mueller, T.; Toher, C.; Curtarolo, S. Machine learning for alloys. *Nat. Rev. Mater.* **2021**, *6*, 730–755. [[CrossRef](#)]
101. Wen, C.; Zhang, Y.; Wang, C.; Xue, D.; Bai, Y.; Antonov, S.; Dai, L.; Lookman, T.; Su, Y. Machine learning assisted design of high entropy alloys with desired property. *Acta Mater.* **2019**, *170*, 109–117. [[CrossRef](#)]
102. Zhang, J.Y.; Zhou, Z.Q.; Zhang, Z.B.; Park, M.H.; Yu, Q.; Li, Z.; Ma, J.; Wang, A.D.; Huang, H.G.; Song, M.; et al. Recent development of chemically complex metallic glasses: From accelerated compositional design, additive manufacturing to novel applications. *Mater. Futures* **2022**, *1*, 12001. [[CrossRef](#)]
103. Zhu, Q.; Zhang, F.; Huang, Y.; Xiao, H.; Zhao, L.; Zhang, X.; Song, T.; Tang, X.; Li, X.; He, G.; et al. An all-round AI-Chemist with scientific mind. *Natl. Sci. Rev.* **2022**, *9*, nwac190. [[CrossRef](#)] [[PubMed](#)]

Disclaimer/Publisher’s Note: The statements, opinions and data contained in all publications are solely those of the individual author(s) and contributor(s) and not of MDPI and/or the editor(s). MDPI and/or the editor(s) disclaim responsibility for any injury to people or property resulting from any ideas, methods, instructions or products referred to in the content.